

Recovery under Side Constraints

Khaled Ardah^{*1}, Martin Haardt^{†2}, Tianyi Liu^{‡3}, Frederic Matter^{§4},
Marius Pesavento^{¶5}, and Marc E. Pfetsch^{||6}

^{1,2}Communications Research Laboratory, Ilmenau University of
Technology, Helmholtzplatz 2, 98684 Ilmenau, Germany

^{3,5}Dept. of Electrical Engineering and Information Technology, TU
Darmstadt, Merckstrasse 25, 64283 Darmstadt, Germany

^{4,6}Department of Mathematics, TU Darmstadt, Dolivostr. 15, 64293
Darmstadt, Germany

February 11, 2022

Abstract

This chapter addresses sparse signal reconstruction under various types of structural side constraints with applications in multi-antenna systems. Side constraints may result from prior information on the measurement system and the sparse signal structure. They may involve the structure of the sensing matrix, the structure of the non-zero support values, the temporal structure of the sparse representation vector, and the nonlinear measurement structure. First, we demonstrate how a priori information in form of structural side constraints influence recovery guarantees (null space properties) using ℓ_1 -minimization. Furthermore, for constant modulus signals, signals with row-, block- and rank-sparsity, as well as non-circular signals, we illustrate how structural prior information can be used to devise efficient algorithms with improved recovery performance and reduced computational complexity. Finally, we address the measurement system design for linear and nonlinear measurements of sparse signals. Moreover, we discuss the linear mixing matrix design based on coherence minimization. Then we extend our focus to nonlinear measurement systems where we design parallel optimization algorithms to efficiently compute stationary points in the sparse phase retrieval problem with and without dictionary learning.

^{*}khaled.ardah@tu-ilmenau.de

[†]martin.haardt@tu-ilmenau.de

[‡]tliu@nt.tu-darmstadt.de

[§]matter@mathematik.tu-darmstadt.de

[¶]pesavento@nt.tu-darmstadt.de

^{||}pfetsch@mathematik.tu-darmstadt.de

1 Introduction

Compressed sensing (CS) is a signal processing technique for efficient acquisition and reconstruction of signals based on an underlying model sparsity, which allows to recover the signal of interest from far fewer samples than required by traditional acquisition systems operating at Nyquist rate. Theoretical recovery guarantees on the number of observations required can be further enhanced if side information on the measurement system and the signal representation is incorporated in form of additional side constraints that are enforced in the recovery process. The measurement system may be subject to various types of side constraints that can be exploited and may originate from *i)* the structure of the sensing matrix (shift-invariance, block structure, sparse co-array structures [48], etc.), *ii)* the structure of the sparse representation vector (integrality, variable bounds, unit-modulus, etc.), *iii)* the sparsity structure in the multiple snapshot case (block or group sparsity, rank sparsity, etc.), as well as *iv)* the structure of the measurements (quantization effects, K-bit measures, magnitude-only measurements, etc.). A fundamental question that arises in this context is, in which sense structural information can be incorporated into the CS problem and how it affects existing algorithms and theoretical results.

Moreover, recovery from nonlinear measurements with sparse models has recently been investigated, e.g., in the classical phase-retrieval problem, where different forms of redundancy have been incorporated through the use of known or unknown linear mixing networks. Redundancy can further enhance recovery in this case.

A large variety of applications involve data recorded from large-scale sensor arrays or *massive multiple-input-multiple output* (MIMO) arrays, which consist of an assembly of wideband sensors to meet the corresponding high throughput and resolution requirements. In this context, sparsity naturally arises in the angular domain, e.g., in form of discrete propagation models and a small number of impinging waveforms from different directions. Similarly, in sensor array and MIMO applications, the structure of the array, the properties of the constellation signal and the transmitted waveform provide important prior information. In order to keep hardware costs in these large scale systems at a reasonable scale while retaining high performance, mixed analog-digital sensing system designs are employed to reduce the number and the sampling rates of the analog-to-digital converters as well as the quality requirements (e.g., w.r.t. linearity, dynamic range, etc.) of the hardware components.

This chapter reviews recent developments on sparse recovery guarantees and efficient recovery algorithms in CS networks under the aforementioned side constraints in the context of multi-antenna systems. First, CS with linear and nonlinear measurement models and the corresponding recovery problems are introduced in Section 2. Theoretical results on the recoverability of linear CS measurements under side constraints are presented in Section 3. Recovery algorithms for sparse measurements under side constraints are addressed in Section 4, and linear mixing matrix design is studied in Section 5. Finally, phase retrieval for known and unknown dictionaries is discussed in Section 6, before conclusions are drawn in Section 7.

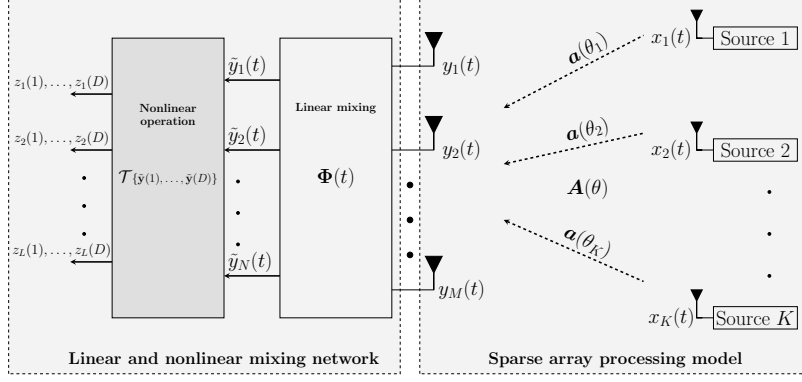


Figure 1: Sparse array processing model with linear and nonlinear mixing network.

2 Sparse Recovery in Sensor Arrays

Consider, as one prominent example application, the following sparse one-dimensional narrow-band array processing model that is frequently encountered in the context of direction-of-arrival (DoA) estimation [26, 61, 15, 4, 2, 47] and multiple-input-multiple output (MIMO) communication [13] and that will be used as a generic example in subsequent sections. We assume that K far-field narrow-band source signals impinge on a sensor array composed of M omni-directional sensors as depicted in the right-hand side of Fig. 1. The t -th time sample of the array output vector $\mathbf{y}(t) = [y_1(t), \dots, y_M(t)]^T \in \mathbb{C}^M$ is given by

$$\mathbf{y}(t) = \mathbf{A}(\boldsymbol{\theta}^{(0)}) \mathbf{x}^{(0)}(t) + \mathbf{n}(t), \quad t = 1, \dots, D, \quad (1)$$

where $\mathbf{x}^{(0)}(t) = [x_1^{(0)}(t), \dots, x_K^{(0)}(t)]^T \in \mathbb{C}^K$ is the vector of waveforms emitted by the K sources, $\mathbf{n}(t) \in \mathbb{C}^M$ contains the spatially and temporally white circular Gaussian sensor noise, and D is the number of available time samples. The matrix $\mathbf{A}(\boldsymbol{\theta}^{(0)}) = [\mathbf{a}(\theta_1), \dots, \mathbf{a}(\theta_K)] \in \mathbb{C}^{M \times K}$ denotes the true array steering matrix, whose i -th column is the array response vector $\mathbf{a}(\theta_i)$ corresponding to the i -th source with DoA $\theta_i \in \Theta$, where Θ defines the field of view. The steering vector $\mathbf{a}(\theta)$ describes a manifold denoted as \mathbb{M}^M . For example, for a uniform linear array (ULA) with half-wavelength inter-element spacing, $\mathbf{a}(\theta)$ is given by $\mathbf{a}(\theta) = [1, e^{-j\pi \sin(\theta)}, \dots, e^{-j(M-1)\pi \sin(\theta)}]^T$. We denote $\boldsymbol{\theta}^{(0)} = [\theta_1^{(0)}, \dots, \theta_K^{(0)}]^T$ as the true DoA parameter vector.

2.1 Compressive Data Model for Sensor Arrays

The model in (1) presumes a dedicated radio frequency (RF) receiver chain for each individual antenna element including an LNA, filters, down-conversion, analog-to-digital converter (ADC), etc. In many applications, however, such separate RF chains for each antenna element come at a high cost in terms of the overall receiver complexity and power consumption. To reduce the number of RF channels (and time samples) without loss in the array aperture, compressed sensing can be applied, where the antenna outputs are linearly combined in the analog domain and then

passed through a reduced number of RF chains to obtain the digital baseband signals as illustrated in the left-hand side of Fig. 1. This can be realized in hardware, e.g., by using configurable hardware components such as tunable phase shifters, a bank of fixed analog beamformers combined with a fast switching network that enables analog beamformer selection, and/or a bank of (tunable) bandpass filters. This way, $N \leq M$ RF receiver channels are used for signal processing in the digital domain.

Let $\Phi^{(0)}(t) \in \mathbb{C}^{N \times M}$ denote the complex analog mixing matrix of a compressive array at time t , which compresses the output of M antenna elements to N active RF channels. Then, the complex (baseband) array output (1) after combining can be expressed as

$$\tilde{\mathbf{y}}(t) = \Phi^{(0)}(t) (\mathbf{A}(\theta^{(0)}) \mathbf{x}^{(0)}(t) + \mathbf{n}(t)) + \mathbf{w}(t), \quad t = 1, \dots, D, \quad (2)$$

where $[\Phi^{(0)}(t)]_{n,m} = \alpha_{n,m}(t) \cdot e^{j\varphi_{n,m}(t)}$, $n = 1, \dots, N$, $m = 1, \dots, M$ with $\alpha_{n,m}(t) \in [0, 1]$, $\varphi_{n,m}(t) \in [0, 2\pi]$, and $\mathbf{w}(t) \in \mathbb{C}^N$ contains the spatially and temporally white circular Gaussian measurement noise. Signals may be subject to additive noise that acts before (i.e., in form of $\mathbf{n}(t)$) or after the mixing network (i.e., in form of $\mathbf{w}(t)$). Defining the effective array steering matrix $\tilde{\mathbf{A}}(\theta^{(0)}, t) = \Phi^{(0)}(t) \mathbf{A}(\theta^{(0)})$, Model (2) becomes

$$\tilde{\mathbf{y}}(t) = \tilde{\mathbf{A}}(\theta^{(0)}, t) \mathbf{x}^{(0)}(t) + \tilde{\mathbf{n}}(t), \quad (3)$$

where $\tilde{\mathbf{n}}(t) = \Phi^{(0)}(t) \mathbf{n}(t) + \mathbf{w}(t)$ is the effective noise vector.

Cost efficient analog hardware devices and data acquisition systems generally involve nonlinear transformations that can perform further compression. Such nonlinear transformations are indicated by the operator \mathcal{T} , which performs a nonlinear mapping from $\mathbb{C}^{N \times D}$ to $\mathbb{C}^{L \times D}$ as depicted in Fig. 1. The types of nonlinearity consist, for instance, of nonlinear transformations introduced from low-cost power amplifiers, magnitude-only and subband power measurements that are often used in cellular communications, C -bit quantization, the more aggressive 1-bit quantization (sign-only measurements), hard-thresholding, and soft-thresholding, or modulo operations. Considering the D time samples simultaneously, the resulting measurement matrix $\mathbf{Z} = [\mathbf{z}(1), \dots, \mathbf{z}(D)] \in \mathbb{C}^{L \times D}$ recorded at the output of the nonlinear mixing network is given by

$$\mathbf{Z} = \mathcal{T} \{ \Phi^{(0)}(1) \mathbf{A}(\theta^{(0)}) \mathbf{x}^{(0)}(1), \dots, \Phi^{(0)}(D) \mathbf{A}(\theta^{(0)}) \mathbf{x}^{(0)}(D) \} + \mathbf{N}, \quad (4)$$

where $\mathbf{N} \in \mathbb{C}^{L \times D}$ combines the various noise contributions. If the mixing matrix $\Phi^{(0)}(t)$ is time-invariant, i.e., $\Phi^{(0)}(t) = \Phi^{(0)}$, the model (4) reduces to

$$\mathbf{Z} = \mathcal{T} \{ \Phi^{(0)} \mathbf{A}(\theta^{(0)}) \mathbf{X}^{(0)} \} + \mathbf{N}, \quad (5)$$

where $\mathbf{X}^{(0)} = [\mathbf{x}^{(0)}(1), \dots, \mathbf{x}^{(0)}(D)] \in \mathbb{C}^{K \times D}$ comprises the D time snapshots.

2.2 Sparse Recovery Formulations for Sensor Arrays

Based on (5), we aim to solve the sparse recovery problem that allows for a robust and efficient estimation of the frequencies of the K sources $x_k^{(0)}(t)$ from the set of measurements $\mathbf{z}(t)$ while exploiting potential structure in $\Phi(t)$, $\tilde{\mathbf{A}}$, \mathbf{A} , and $\mathbf{x}^{(0)}(t)$, or specific properties of \mathcal{T} . Specifically, we will address variations of the general multiple measurement $\ell_{p,q}$ mixed-norm minimization problem

$$\min_{\mathbf{X}, \Phi} \frac{1}{2} \|\mathbf{Z} - \mathcal{T} \{ \Phi \mathbf{A}(\theta) \mathbf{X} \} \|_{\text{F}}^2 + \lambda \|\mathbf{X}\|_{p,q} : \text{side constraints}, \quad (\text{P0})$$

where at this point Φ is assumed to be time-invariant for simplicity of description (i.e., considering (5)), $\mathbf{A}(\theta) \in \mathbb{C}^{M \times P}$ with $P \gg M$ is a “fat” sensing matrix corresponding to the P -dimensional DoA grid vector θ that appropriately samples the field of view Θ , and $\mathbf{X} \in \mathbb{C}^{P \times D}$ is the row sparse (joint sparse) signal matrix of interest, i.e., its columns share the same support. The support of the non-zero rows of \mathbf{X} corresponds to the DoAs on the spatial grid. Moreover, the regularization parameter $\lambda > 0$ controls the trade-off between the data fitting term and the sparsity level in \mathbf{X} . The joint sparsity in \mathbf{x} is induced by the $\ell_{p,q}$ mixed-norm defined as

$$\|\mathbf{X}\|_{p,q} = \left(\sum_{k=1}^P \|\mathbf{x}_k\|_p^q \right)^{1/q}, \quad (6)$$

for $p, q \geq 1$, which applies an inner ℓ_p norm to the rows \mathbf{x}_k , $k = 1, \dots, P$ in $\mathbf{X} = [\mathbf{x}_1, \dots, \mathbf{x}_P]^T$ and an outer ℓ_q norm to the ℓ_p row-norms. Ideally, we aim to solve (P0) using the $\ell_{p,0}$ pseudo-norm $\|\mathbf{X}\|_{p,0}$, which is the cardinality of the nonzero ℓ_p -norms of the rows of \mathbf{X} . If $D = 1$, the model reduces to the single measurement case and the $\ell_{p,1}$ mixed-norm reduces to the ℓ_1 norm.

In the absence of the various noise contributions, i.e., $\mathbf{N} = \mathbf{0}$, the general minimization problem (P0) can be equivalently written as

$$\min_{\mathbf{X}, \Phi} \{ \|\mathbf{X}\|_{p,q} : \mathcal{T} \{ \Phi \mathbf{A}(\theta) \mathbf{X} \} = \mathbf{Z}, \text{ additional side constraints} \}. \quad (7)$$

3 Recovery Guarantees under Side Constraints

In this section, we consider the uniform recovery of sparse solutions with additional side constraints on the solutions/signals. We use the signal model (1) without noise in the single measurement case, i.e., $\mathbf{n} = \mathbf{0}$ and $D = 1$. More precisely, consider the equation system $\mathbf{A}\mathbf{x} = \mathbf{y}$ for $\mathbf{A} \in \mathbb{R}^{m \times n}$, $\mathbf{y} \in \mathbb{R}^m$. The side constraints for \mathbf{x} can be expressed by requiring that $\mathbf{x} \in C \subseteq \mathbb{R}^n$. This leads to optimization models

$$\min \{ \|\mathbf{x}\|_0 : \mathbf{A}\mathbf{x} = \mathbf{y}, \mathbf{x} \in C \}, \quad (8)$$

i.e., variants of (7) in the single measurement case without nonlinearities, which promise to be able to uniquely recover sparse solutions for a larger set of right hand side vectors \mathbf{y} . This is illustrated by the following very simple toy example.

Example 1 Consider the following recovery problem for $n = 2$. Let $\mathbf{A} = [1, -1]$ and $y = 1$. The system $\mathbf{A}\mathbf{x} = y$ has two sparse solutions, namely $\mathbf{x}_1 = (1, 0)^T$ and $\mathbf{x}_2 = (0, -1)^T$. Since $\|\mathbf{x}_1\|_1 = \|\mathbf{x}_2\|_1 = 1$, it is not possible to uniquely recover either point by ℓ_1 -minimization, nor by ℓ_0 -minimization. But by exploiting nonnegativity, \mathbf{x}_1 can indeed be uniquely recovered.

Another example of a whole family of sensing matrices showing that exploiting side constraints leads to weaker recovery conditions can be found in [19, Theorem 4.5]. This shows that side constraints are not only of theoretical interest, but should be exploited in the recovery process. The price to pay may of course be that the recovery problems become harder to solve.

3.1 Integrality Constraints

One particular example of an interesting side constraint is the integrality of \mathbf{x} . Applications include discrete tomography [29] or massive MIMO with constellation signals [17, 18]. A notable special case of this setting includes the recovery of binary vectors, which has applications in digital or wireless communication systems.

The corresponding general recovery problem can be formulated as

$$\min \{\|\mathbf{x}\|_0 : \mathbf{Ax} = \mathbf{Ax}^{(0)}, \mathbf{x} \in [\boldsymbol{\ell}, \mathbf{u}]_{\mathbb{Z}}\}, \quad (9)$$

where $\mathbf{x}^{(0)} \in [\boldsymbol{\ell}, \mathbf{u}]_{\mathbb{Z}} := \{\mathbf{x} \in \mathbb{Z}^n : \ell_i \leq x_i \leq u_i, i \in [n]\}$ is an s -sparse vector and $\mathbf{A} \in \mathbb{R}^{m \times n}$. Note that we can assume $\boldsymbol{\ell} \in \mathbb{Z}^n \cup \{-\infty\}$ and $\mathbf{u} \in \mathbb{Z}^n \cup \{\infty\}$. As in the case of classical sparse recovery, we consider the ℓ_1 -relaxation of (9), namely

$$\min \{\|\mathbf{x}\|_1 : \mathbf{Ax} = \mathbf{Ax}^{(0)}, \mathbf{x} \in [\boldsymbol{\ell}, \mathbf{u}]_{\mathbb{Z}}\}. \quad (10)$$

In the literature, recovery of binary and integral sparse vectors using (10) has been considered for example in [22, 53], where the nonconvex integrality condition was relaxed to $\mathbf{x} \in [\boldsymbol{\ell}, \mathbf{u}] := \{\mathbf{x} \in \mathbb{R}^n : \boldsymbol{\ell} \leq \mathbf{x} \leq \mathbf{u}\}$. In this case, the integrality assumption does not help for recovery: uniform recovery of all sparse bounded integral \mathbf{x} is equivalent to uniform recovery of all sparse bounded \mathbf{x} , see [22]. This already shows that in order to exploit integrality, one has to take this into account in the recovery program. Note that (10) is nonconvex but can be formulated as a mixed-integer (linear) program (MIP).

It turns out that in case of rational measurement matrices \mathbf{A} and no bounds on the variables, there is again no difference between integral and general \mathbf{x} . However, in the presence of additional bounds, this is no longer true. In this case it is possible to formulate null space properties depending on the bounds $\boldsymbol{\ell}, \mathbf{u}$ that characterize uniform recovery of integral (bounded) sparse vectors \mathbf{x} using (10), see [30]. To this end, define the following two *null space properties* (NSP) depending on a set $V \subseteq \mathbb{R}^n$. Let $\mathbf{A} \in \mathbb{R}^{m \times n}$ and $S \subseteq [n] := \{1, \dots, n\}$ and define

$$\begin{aligned} \text{NSP}(V) : \quad & \|\mathbf{v}_S\|_1 < \|\mathbf{v}_{\bar{S}}\|_1 \quad \forall \mathbf{v} \in (V \cap \mathcal{N}(\mathbf{A})) \setminus \{\mathbf{0}\}, \\ \text{NSP}_+(V) : \quad & \mathbf{v}_{\bar{S}} \leq \mathbf{0} \implies \sum_{i=1}^n v_i < 0 \quad \forall \mathbf{v} \in (V \cap \mathcal{N}(\mathbf{A})) \setminus \{\mathbf{0}\}, \end{aligned}$$

where \bar{S} denotes the complement of a set S , \mathbf{v}_S denotes the vector of elements indexed by S and $\mathcal{N}(\mathbf{A})$ denotes the null space of the matrix \mathbf{A} .

Then, $\text{NSP}(\mathbb{R}^n)$ is the classical null space property [14, 12] which characterizes uniform recovery of sparse vectors \mathbf{x} by ℓ_1 -minimization, and $\text{NSP}_+(\mathbb{R}^n)$ is the well-known nonnegative null space property [23, 77] characterizing uniform recovery via nonnegative ℓ_1 -minimization.

For integral vectors without bounds, i.e., $\ell_i = -\infty$ and $u_i = \infty$ for all $i \in [n]$, and integral nonnegative vectors, the results for uniform recovery are completely analogous to the classical case with the only exception that for satisfying the NSP, only integral vectors in the null space of \mathbf{A} are of interest, see [30] for the exact statements. This observation also shows that for $\mathbf{A} \in \mathbb{Q}^{m \times n}$, the classical (nonnegative) NSP and the corresponding integral (nonnegative) NSP coincide. Thus, for rational data, exploiting integrality does not lead to improved recovery conditions.

If the bounds ℓ , \mathbf{u} are nontrivial, the situation changes fundamentally. The first difference is that for classical recovery, bounds on \mathbf{x} do not influence recovery properties, since vectors in the null space of \mathbf{A} can be scaled accordingly. For integral vectors, however, a new NSP in the presence of bounds $-\infty \leq \ell_i \leq 0 \leq u_i \leq \infty$ for all $i \in [n]$ arises. Then it turns out that the condition $\text{NSP}([\ell - \mathbf{u}, \mathbf{u} - \ell]_{\mathbb{Z}})$ provides a sufficient condition for uniform recovery using (10), but not a characterization. Nevertheless we can use a variable split into positive and negative part to obtain an NSP that characterizes uniform recovery in the following statement.

Theorem 1 ([30]) *Let $\mathbf{A} \in \mathbb{R}^{m \times n}$ and $s \geq 0$. Then every s -sparse vector $\mathbf{x}^{(0)} \in [\ell, \mathbf{u}]_{\mathbb{Z}}$ is the unique solution of (10) if and only if*

$$-(\mathbf{v}_{\bar{S}}, \mathbf{w}_{\bar{S}})^T \in K \implies \sum_{i=1}^n v_i + w_i < 0,$$

holds for all $(\mathbf{v}, \mathbf{w})^T \in \mathcal{N}(\mathbf{A}, -\mathbf{A}) \cap (K + (-K))$ with $(\mathbf{v}, \mathbf{w})^T \neq (\mathbf{0}, \mathbf{0})^T$ and all $S \subseteq [n]$, $|S| \leq s$, where

$$K := \left\{ \begin{pmatrix} \mathbf{x} \\ \mathbf{y} \end{pmatrix} \in \left[\begin{pmatrix} 0 \\ 0 \end{pmatrix}, \begin{pmatrix} \mathbf{u} \\ -\ell \end{pmatrix} \right]_{\mathbb{Z}} : x_i \cdot y_i = 0, i \in [n] \right\}.$$

The complementarity constraints $x_i \cdot y_i = 0$ in K are due to the split into positive and negative part. This already shows that the introduction of bounds leads to different recovery conditions, in contrast to the situation of classical sparse recovery over \mathbb{R}^n . For testing the NSP in Theorem 1, one needs to take care of the complementarity constraints $x_i \cdot y_i = 0$. This can be done by, e.g., using methods from [11, 10]. For nonnegative integral vectors with upper bounds, the variable split is not needed, and it can be shown that $\text{NSP}_+([\mathbf{u}, \mathbf{u}]_{\mathbb{Z}})$ characterizes uniform recovery [30].

Besides using (10) for recovery of sparse integral vectors, one can also use the exact recovery problem (9), which can be formulated as a MIP if there are finite bounds by expressing the nonconvex ℓ_0 -objective using binary variables. In this case it is also possible to characterize when solving (9) recovers any s -sparse integral vector with or without bounds. The condition of classical sparse recovery is $\text{spark}(\mathbf{A}) > 2s$, where $\text{spark}(\mathbf{A})$ denotes the smallest number of linear dependent columns in \mathbf{A} . The corresponding statements for integral sparse recovery appear in [30].

3.2 General Framework for Arbitrary Side Constraints

In the previous section, we have explicitly considered integrality constraints as one specific side constraint that can be exploited in the recovery process. The corresponding recovery conditions resemble the well-known null space properties that exist for various other settings such as sparse (nonnegative) recovery [12, 14, 23, 77], block-sparse recovery [54] or low-rank (positive semidefinite) matrix recovery [24, 37]. Thus it seems reasonable to search for a general setting and null space property that unifies the cases already considered in the literature. Such a general framework is presented in [21] that comprises all the previously mentioned settings but does not handle additional side constraints such as nonnegativity, integrality and positive semidefiniteness. Sparsity in this general framework

is expressed using projections. Recently, this general framework was extended in [19] to also cover additional side constraints. Under mild assumptions on the side constraints and the measurement process it is possible to state an NSP for the corresponding general recovery problem. It turns out that this general NSP specializes to the already known NSPs in the various special cases mentioned above. In the following, we will shortly describe this general recovery framework and provide an application in order to evaluate the influence of side constraints.

For the general framework, we need two finite-dimensional Euclidean spaces \mathcal{X} and \mathcal{E} . A *linear sensing map* $A: \mathcal{X} \rightarrow \mathbb{R}^m$ is used for acquiring signals $x \in \mathcal{X}$ and a *linear representation map* $B: \mathcal{X} \rightarrow \mathcal{E}$ is used for mapping a signal to an appropriate representation. We will denote the image of x under a linear operator F as Fx . Additional side constraints are modeled using a set $C \subseteq \mathcal{X}$ with $0 \in C$. The image of C under the map B is denoted with \mathcal{D} . Finally, let $\|\cdot\|$ be a norm on \mathcal{E} .

Sparsity in this general framework is expressed using projections onto appropriate subspaces. Therefore, let \mathcal{P} be a set of matrices representing linear maps on \mathcal{E} . Each $P \in \mathcal{P}$ is assigned a nonnegative real weight by $\nu: \mathcal{P} \rightarrow \mathbb{R}_+$ and a linear map $\bar{P}: \mathcal{E} \rightarrow \mathcal{E}$. Then, for $s \in \mathbb{R}_+$, an element $\mathbf{x} \in \mathcal{X}$ is called *s-sparse*, if there exists a linear map $P \in \mathcal{P}$ with $\nu(P) \leq s$ and $PB\mathbf{x} = B\mathbf{x}$. Furthermore, let $\mathcal{P}_s = \{P \in \mathcal{P} : \nu(P) \leq s\}$ be the set of linear maps that allow *s-sparse* elements.

The corresponding generalized recovery problem for a given right-hand side $\mathbf{y} \in \mathbb{R}^m$ can be formulated as

$$\min \{\|B\mathbf{x}\| : A\mathbf{x} = \mathbf{y}, \mathbf{x} \in C\}. \quad (11)$$

Note that this is convex if C is convex. Using this general framework, it is possible to state two NSPs that can be used to characterize uniform recovery using the general recovery problem (11).

Definition 1 *The linear sensing map A satisfies the general null space property of type I and type II of order s for the set C if and only if for all $\mathbf{v} \in (\mathcal{N}(A) \cap (C + (-C)))$ with $B\mathbf{v} \neq \mathbf{0}$ and all $P \in \mathcal{P}_s$ it holds that*

$$\begin{aligned} -\bar{P}B\mathbf{v} \in \mathcal{D} &\implies \exists \mathbf{v}^{(1)}, \mathbf{v}^{(2)} \in C, \mathbf{v} = \mathbf{v}^{(1)} - \mathbf{v}^{(2)}, \|PB\mathbf{v}^{(1)}\| - \|PB\mathbf{v}^{(2)}\| < \|\bar{P}B\mathbf{v}\|, \\ &\quad \text{(NSP-I}^C\text{)} \\ -\bar{P}B\mathbf{v} \in \mathcal{D} &\implies \forall \mathbf{v}^{(1)}, \mathbf{v}^{(2)} \in C, \mathbf{v} = \mathbf{v}^{(1)} - \mathbf{v}^{(2)}, \|PB\mathbf{v}^{(1)}\| - \|PB\mathbf{v}^{(2)}\| < \|\bar{P}B\mathbf{v}\|, \\ &\quad \text{(NSP-II}^C\text{)} \end{aligned}$$

respectively, where $\mathcal{N}(A) := \{\mathbf{v} \in \mathcal{X} : A\mathbf{v} = \mathbf{0}\}$ is the null space of A .

Example 2 (Recovery of sparse nonnegative vectors by ℓ_1 -minimization) *For the recovery of nonnegative vectors let $\mathcal{X} = \mathcal{E} = \mathbb{R}^n$, B be the identity and $\|\cdot\| = \|\cdot\|_1$. The set of side constraints is $C = \mathbb{R}_+^n$, implying $\mathcal{D} = \mathbb{R}_+^n$. Let \mathcal{P} be the set of orthogonal projectors onto all coordinate subspaces of \mathbb{R}^n , and define $\bar{P} := I_n - P$, where I_n denotes the identity mapping on \mathbb{R}^n . Define the nonnegative weight $\nu(P) := \text{rk}(P)$, so that $\nu(P)$ is the number of nonzero components of the subspace P projects onto. The notion of general sparsity reduces to the classical sparsity of nonzero entries in a vector $\mathbf{x} \in \mathbb{R}_+^n$ and the recovery problem (11) becomes nonnegative ℓ_1 -minimization with $PB\mathbf{x} = \mathbf{x}_S$ and $\bar{P}B\mathbf{x} = \mathbf{x}_{\bar{S}}$. In this case, it can be shown that the general null space property (NSP-I^C) of order s for the set C is equivalent to the known nonnegative null space property [23, 77]*

$$\mathbf{v}_{\bar{S}} \leq 0 \implies \sum_{i \in S} v_i < \|\mathbf{v}_{\bar{S}}\|_1, \forall \mathbf{v} \in \mathcal{N}(A) \setminus \{\mathbf{0}\}, \forall S \subseteq [n], |S| \leq s, \text{ (NSP}_{\geq 0}\text{)}$$

where S denotes the index set of components on which P projects.

Under mild assumptions, the null space properties (NSP-I^C) and (NSP-II^C) can be proven to characterize uniform recovery using (11). Which NSP is needed depends on which assumptions are satisfied. For the formal statement and more examples of how the various settings already considered in the literature turn out to be special cases of this general recovery statement, see [19]. At this point it is important to notice that already in the special case of sparse vectors, checking whether \mathbf{A} satisfies the classical NSP is \mathcal{NP} -hard [57].

The two NSPs characterizing uniform recovery in a very general framework already indicate that a stronger, i.e., more restrictive side constraint leads to weaker conditions that need to be satisfied to guarantee uniform recovery.

In [19] an NSP for the recovery of positive semidefinite block-diagonal matrices is derived, which has not been considered before. Let $\mathbf{X} \in \mathcal{S}_+^n$ be a (symmetric) positive semidefinite matrix and $\mathcal{A}: \mathcal{S}^n \rightarrow \mathbb{R}^m$, $\mathcal{A}(\mathbf{X}) = (\mathbf{A}_1 \bullet \mathbf{X}, \dots, \mathbf{A}_m \bullet \mathbf{X})^T$ be a linear operator, where $\mathbf{A}_1, \dots, \mathbf{A}_m \in \mathcal{S}^n$ are symmetric matrices and “ \bullet ” denotes the componentwise inner product. In order to define a block-diagonal form, let $k \geq 1$ and $B_1, \dots, B_k \neq \emptyset$ be a partition of $[n]$. The matrix \mathbf{X} and the linear measurement operator $\mathcal{A}(\mathbf{X})$ are in *block-diagonal form* with blocks B_1, \dots, B_k , if $X_{s,t} = (A_i)_{s,t} = 0$ for all $(s,t) \notin (B_1 \times B_1) \cup \dots \cup (B_k \times B_k)$ and all $i \in [m]$. Let \mathbf{X}_B be the submatrix containing rows and columns of \mathbf{X} indexed by B . The corresponding norm is given by the $\ell_{*,q}$ -norm defined as

$$\|\mathbf{X}\|_{*,q} := \|(\|\mathbf{X}_{B_1}\|_*, \dots, \|\mathbf{X}_{B_k}\|_*)^T\|_q,$$

and the block-support $\text{BS}(\mathbf{X})$ is given by the indices of those blocks $\mathbf{X}_{B_i} \neq \mathbf{0}$. By using an appropriate linear representation map to encode the block-diagonal structure, (NSP-I^C) simplifies to

$$\mathbf{V}_{B_i} \leq 0 \quad \forall i \in \bar{S} \quad \implies \quad \sum_{i \in S} \mathbf{1}^T \lambda(\mathbf{V}_{B_i}) < \sum_{i \in \bar{S}} \|\mathbf{V}_{B_i}\|_*, \quad (\text{NSP}_{*,1,\geq 0}^*)$$

for all $\mathbf{V} \in (\mathcal{N}(\mathbf{A}) \cap \mathcal{S}^n) \setminus \{\mathbf{0}\}$ and all $S \subseteq [k]$, $|S| \leq s$, where $\lambda(\mathbf{V}_{B_i})$ is the vector of eigenvalues of \mathbf{V}_{B_i} , and $\mathbf{1}$ is a vector of ones. The general uniform recovery statement [19, Theorem 2.7] yields the following theorem.

Theorem 2 ([19]) *Let $\mathbf{A}(\mathbf{X})$ be a linear operator in block-diagonal form and $s \geq 1$. Then, every positive semidefinite $\mathbf{X}^{(0)} \in \mathcal{S}_+^n$ with $\|\mathbf{X}^{(0)}\|_{*,0} \leq s$ is the unique solution of $\min \{\|\mathbf{X}\|_{*,1} : \mathbf{A}(\mathbf{X}) = \mathbf{A}(\mathbf{X}^{(0)}), \mathbf{X} \geq 0\}$ if and only if $\mathbf{A}(\mathbf{X})$ satisfies (NSP_{*,1,\geq 0}^*) of order s .}*

As a conclusion, the general framework presented above can answer many interesting questions concerning uniform recovery in the presence of side constraints using the optimization problem (11). The two general null space properties (NSP-I^C) and (NSP-II^C) can be used to analyze and quantify the exact impact of various side constraints in the recovery process. Given a specific setting, the NSPs can decide whether additional side information is needed or which side constraints need to be exploited in the recovery process to guarantee uniform recovery. For instance, this framework explains why there are two seemingly different NSP formulations for classical sparse recovery and nonnegative sparse recovery and their connection.

4 Recovery Algorithms Under Different Side Constraints for the Linear Measurement Model

4.1 Constant Modulus Constraints

In this section we consider a variation of Problem (8) for the case of noisy measurements \mathbf{s} and for side constraints on the sparse representation vector of the form $\{\mathbf{x} \in \mathbb{C}^N : |x_n| \in \{0, c\} \forall n \in [N]\}$. This problem emerges, e.g., in multi-user massive MIMO hybrid precoding systems with antenna selection and strict per antenna magnitude requirements [9]. In this application, let \mathbf{A} denote the MIMO $N \times K$ channel matrix, \mathbf{y} denote the symbol vector of the K users, and \mathbf{x} denote the transmitted signal vector. To limit nonlinearity effects in the power amplifiers, the magnitudes of nonzero signals x_n transmitted from the selected antennas are restricted to a constant c . The optimization problem can be formulated as [9]:

$$\min_{\mathbf{x} \in \mathbb{C}^N} \|\mathbf{x}\|_0 \quad (12a)$$

$$\text{s.t. } \|\mathbf{y} - \mathbf{A}^T \mathbf{x}\|_2 \leq \sqrt{\delta}, \quad (12b)$$

$$|x_n| \in \{0, c\}, \quad \forall n \in [N], \quad (12c)$$

where $\|\mathbf{x}\|_0 = |\{n \in [N] : x_n \neq 0\}|$ denotes the number of nonzero entries of \mathbf{x} , i.e., the number of active antennas. We assume without loss of generality that $c = 1$. In order to reformulate the constant modulus constraint (12c), we split vector \mathbf{x} into real and imaginary part $\text{Re}[\mathbf{x}]$ and $\text{Im}[\mathbf{x}]$, respectively. Let $\mathbf{b} = [b_1, b_2, \dots, b_N]^T \in \{0, 1\}^N$ denote a vector of binary variables. Problem (12) can then be written as

$$\min_{\mathbf{x} \in \mathbb{C}^N, \mathbf{b} \in \{0, 1\}^N} \sum_{n=1}^N b_n \quad (13a)$$

$$\text{s.t. } \sum_{k=1}^K \left(\text{Re}[y_k] - (\text{Re}[\mathbf{a}_k]^T \mathbf{w} - \text{Im}[\mathbf{a}_k]^T \mathbf{z}) \right)^2 + \left(\text{Im}[y_k] - (\text{Re}[\mathbf{a}_k]^T \mathbf{z} + \text{Im}[\mathbf{a}_k]^T \mathbf{w}) \right)^2 \leq \delta, \quad (13b)$$

$$\text{Re}[x_n]^2 + \text{Im}[x_n]^2 \leq b_n, \quad \forall n \in [N], \quad (13c)$$

$$\text{Re}[x_n]^2 + \text{Im}[x_n]^2 \geq b_n, \quad \forall n \in [N], \quad (13d)$$

$$b_n \in \{0, 1\}, \quad \forall n \in [N]. \quad (13e)$$

In (13) we have replaced the modulus constraints $|x_n|^2 = \text{Re}[x_n]^2 + \text{Im}[x_n]^2 = b_n$, $n \in [N]$, by the two inequality constraints (13c) and (13d), which will be treated differently in the following. The mixed-integer nonlinear program (13) will be solved by employing a spatial branching method [62] in which branching is performed both on integral as well as continuous variables. In this branch-and-bound procedure the binary constraints $b_n \in \{0, 1\}$ at each node of the tree are relaxed to linear inequality constraints $0 \leq b_n \leq 1$.

In the case that the solution $(\hat{\mathbf{x}}, \hat{\mathbf{b}})$ of the LP relaxation of Problem (13) does not satisfy the condition $\text{Re}[x_n]^2 + \text{Im}[x_n]^2 \geq b_n$ for some $n \in [N]$, this constraint violation will be resolved by one of the following steps:

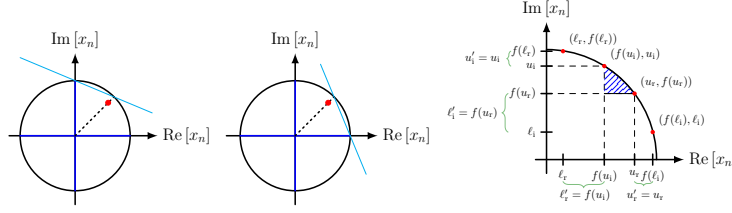


Figure 2: Left: Inequalities that are added to the sub-nodes, Right: Bound propagation for the continuous variables.

1. If the binary variable \hat{b}_n is already fixed to zero, the inequality $\text{Re}[x_n]^2 + \text{Im}[x_n]^2 \leq b_n$ implies that also \hat{x}_n is set to zero.
2. If the bounds of the continuous variables $\text{Re}[x_n]$ and $\text{Im}[x_n]$ are not yet restricted to one of the orthants w.r.t. $\text{Re}[x_n] \times \text{Im}[x_n]$, four branching nodes can be created, the first with the additional constraints $\text{Re}[x_n] \geq 0$, $\text{Im}[x_n] \geq 0$, the second with $\text{Re}[x_n] \geq 0$, $\text{Im}[x_n] \leq 0$, the third with $\text{Re}[x_n] \leq 0$, $\text{Im}[x_n] \leq 0$, and the fourth with $\text{Re}[x_n] \leq 0$, $\text{Im}[x_n] \geq 0$. This partitions the feasible solution set into these four orthants.
3. If the bounds of the continuous variables $\text{Re}[x_n]$ and $\text{Im}[x_n]$ are already restricted to one of these four orthants, the following steps are performed. Assume w.l.o.g. that (\hat{x}_n, \hat{b}_n) is feasible for the first orthant, i.e., the one with $\text{Re}[x_n] \geq 0$ and $\text{Im}[x_n] \geq 0$.

Propagation: Let $\ell_r \leq \text{Re}[x_n] \leq u_r$, $\ell_i \leq \text{Im}[x_n] \leq u_i$ denote the current lower and upper bounds of the variables $\text{Re}[x_n]$ and $\text{Im}[x_n]$, respectively. Compute the four points $(\ell_r, f(\ell_r))$, $(u_r, f(u_r))$, $(f(\ell_i), \ell_i)$ and $(f(u_i), u_i)$ on the unit circle that correspond to the respective lower and upper bounds of $\text{Re}[x_n]$ and $\text{Im}[x_n]$, where $f(x) = \sqrt{1-x^2}$. These four points can now be used to strengthen the lower and upper bounds of $\text{Re}[x_n]$ and $\text{Im}[x_n]$. In order for an optimal solution $(\mathbf{x}^*, \mathbf{b}^*)$ to fulfill the modulus constraint $\text{Re}[x_n]^2 + \text{Im}[x_n]^2 \geq b_n$, the point $(\text{Re}[x_n^*], \text{Im}[x_n^*])$ needs to lie on or above the arc between the two points (ℓ'_r, u'_i) and (u'_r, ℓ'_i) if $b_n^* = 1$, where $\ell'_r = \max\{\ell_r, f(u_i)\}$, $u'_r = \min\{u_r, f(\ell_i)\}$, $\ell'_i = \max\{\ell_i, f(u_r)\}$, $u'_i = \min\{u_i, f(\ell_r)\}$. This implies that the four values ℓ'_r , u'_r , ℓ'_i and u'_i can now be taken as new and possibly strengthened lower and upper bounds of $\text{Re}[x_n]$ and $\text{Im}[x_n]$, respectively. If the binary variable b_n is not yet fixed to one, the lower bounds are not propagated, as b_n could be set to zero in an optimal solution, implying $\text{Re}[x_n] = \text{Im}[x_n] = 0$ as well. A visualization of this propagation is given in the right hand side of Fig. 2.

Separation: If $\text{Re}[\hat{x}_n] + \text{Im}[\hat{x}_n] < \hat{b}_n$, add the cut $\text{Re}[x_n] + \text{Im}[x_n] \geq b_n$ to the LP relaxation. Note that each solution in this orthant on the unit circle satisfies this inequality.

Branching: If $\text{Re}[\hat{x}_n] + \text{Im}[\hat{x}_n] \geq \hat{b}_n$, create two branching nodes defined by inequalities $f_n \text{Re}[x_n] + g_n \text{Im}[x_n] \geq b_n$, where $f_n \in \mathbb{R}$ and $g_n \in \mathbb{R}$ can be computed according to the left hand side of Fig. 2.

Computationally efficient suboptimal heuristic solutions for problem (12) and simulation results from numerical experiments can further be found in [9].

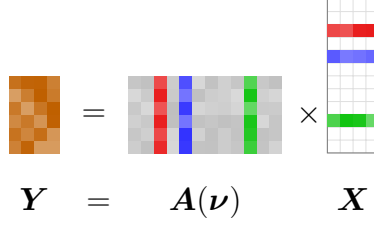


Figure 3: Multiple measurement problem with row-sparsity.

4.2 Row and Rank Sparsity

In this section we consider row and rank sparse recovery from noisy measurements. The idea to exploit a common sparsity structure among multiple measurements as prior information was proposed in [75, 58, 60, 25, 36, 20], where the mixed-norm (6) is used to enforce row-sparsity. The corresponding row-sparse data model is illustrated in Fig. 3. The classical row-sparse recovery problem corresponds to a least-squares data fitting problem with $\ell_{2,1}$ mixed-norm minimization:

$$\min_{\mathbf{X}} \frac{1}{2} \|\mathbf{A}\mathbf{X} - \mathbf{Y}\|_F^2 + \lambda \sqrt{D} \|\mathbf{X}\|_{2,1}, \quad (14)$$

where $\mathbf{X} = [\mathbf{x}(1), \dots, \mathbf{x}(D)]$. This problem emerges, e.g., in the context of Direction-of-Arrival (DoA) estimation, where the columns of the dictionary \mathbf{A} represent the array responses for difference directions and the support of the matrix \mathbf{X} , i.e., the indices of the non-zero rows indicate the source DoAs. The dimension of problem (14) grows with the number of measurements D and the size of the dictionary and can become computationally intractable. To reduce the computational cost it was suggested in [36] to reduce the dimension of the $M \times D$ measurement matrix \mathbf{Y} by matching only the signal subspace in form of an $M \times K$ matrix \mathbf{Y}_{SV} , leading to the prominent ℓ_1 -SVD method. A drawback of the ℓ_1 -SVD method is that it requires knowledge of the number of source signals and that the estimation performance may deteriorate in the case of correlated source signals. To overcome this limitation a convenient equivalent problem reformulation was derived in [43] as stated in the following theorem.

Theorem 3 (Problem Equivalence 1) *The row-sparsity inducing $\ell_{2,1}$ mixed-norm minimization problem (14) is equivalent to the convex problem*

$$\min_{\mathbf{S} \in \mathbb{D}_+} \text{tr}((\mathbf{A}\mathbf{S}\mathbf{A}^H + \lambda \mathbf{I}_M)^{-1} \hat{\mathbf{R}}) + \text{tr}(\mathbf{S}), \quad (15)$$

with $\hat{\mathbf{R}} = \mathbf{Y}\mathbf{Y}^H/D$ denoting the sample covariance matrix and \mathbb{D}_+ describing the set of nonnegative diagonal matrices, in the sense that minimizers \mathbf{X}^* and \mathbf{S}^* for problems (14) and (15), respectively, are related by

$$\mathbf{X}^* = \mathbf{S}^* \mathbf{A}^H (\mathbf{A} \mathbf{S}^* \mathbf{A}^H + \lambda \mathbf{I}_M)^{-1} \mathbf{Y}. \quad (16)$$

Conversely, $\mathbf{S}^* = \text{diag}(s_1^*, \dots, s_K^*)$ contains the row-norms of the sparse signal matrix $\mathbf{X}^* = [\mathbf{x}_1^*, \dots, \mathbf{x}_K^*]^T$ on its diagonal according to

$$s_k^* = \frac{1}{\sqrt{D}} \|\mathbf{x}_k^*\|_2, \quad (17)$$

$$\mathbf{Y} = \mathbf{B}(\boldsymbol{\nu}) \boldsymbol{\Phi}(\boldsymbol{\nu}, \boldsymbol{\eta}) \mathbf{X} + \mathbf{N} = \mathbf{B}(\boldsymbol{\nu}) \mathbf{Z} + \mathbf{N}$$

Figure 4: Multiple measurement problem with block-sparsity.

for $k = 1, \dots, K$, such that the union support of \mathbf{X}^* is equivalently represented by the support of the sparse vector of row-norms $[s_1^*, \dots, s_K^*]^T$.

Problem (16) is known as the SPARse ROW-norm reconstruction (SPARROW) reformulation. It reveals several interesting properties of the underlying multiple measurement problem and it can be reformulated as a semidefinite program. Unlike Problem (14) the dimension of (16) does not grow with the number of measurements [43]. Gridless variants of the method for uniform linear arrays (ULAs), shift-invariant arrays and augmentable arrays are reported in [43, 55, 44, 3, 63]. In the case of DoA estimation in partly calibrated subarray systems with unknown DoAs $\boldsymbol{\nu}$ and subarray position parameters $\boldsymbol{\eta}$, the recovery problem can be formulated as a rank- and block-sparse regularization problem [41]. The corresponding data model is illustrated in Fig. 4, where $\mathbf{B}(\boldsymbol{\nu})$ contains the subarray steering vectors, $\boldsymbol{\Phi}(\boldsymbol{\nu}, \boldsymbol{\eta}) = [\boldsymbol{\varphi}(\nu_1, \boldsymbol{\eta}), \dots, \boldsymbol{\varphi}(\nu_K, \boldsymbol{\eta})]$ contains the inter-subarray array responses, and \mathbf{X} contains the row-sparse waveforms. We observe that the matrix $\mathbf{Z} = [\mathbf{Z}_1^T, \dots, \mathbf{Z}_K^T]^T$ enjoys a special block- and rank-sparse structure as it is composed of K stacked rank-one matrices $\mathbf{Z}_k = \boldsymbol{\varphi}(\nu_k, \boldsymbol{\eta}) \mathbf{x}_k^T$, for $k = 1, \dots, K$. The block- and rank-sparse recovery problem is given by

$$\min_{\mathbf{Z}} \frac{1}{2} \|\mathbf{B}\mathbf{Z} - \mathbf{Y}\|_F^2 + \sum_{k=1}^K \|\mathbf{Z}_k\|_*, \quad (18)$$

where the nuclear norm regularization $\|\mathbf{Z}_k\|_* = \text{tr}((\mathbf{Z}_k^H \mathbf{Z}_k)^{1/2})$ encourages block rank sparsity, i.e., the solutions blocks \mathbf{Z}_k shall either be zero or low rank [67, 45, 28, 27]. Similar to Problem (14) also Problem (18) admits a convenient reformulation with a significantly reduced number optimization variables, as provided by the following theorem [41, 42].

Theorem 4 (Problem Equivalence 2) *The rank- and block-sparsity inducing $\ell_{*,1}$ mixed-norm minimization Problem (18) is equivalent to the convex problem*

$$\min_{\mathbf{S} \in \mathcal{S}_K^+} \text{tr}((\mathbf{B}\mathbf{S}\mathbf{B}^H + \lambda \mathbf{I})^{-1} \hat{\mathbf{R}}) + \text{tr}(\mathbf{S}), \quad (19)$$

with $\hat{\mathbf{R}} = \mathbf{Y}\mathbf{Y}^H/D$ and \mathcal{S}_K^+ denoting the sample covariance matrix and the set of positive semidefinite block-diagonal matrices composed of K blocks of size $P \times P$, respectively. The equivalence holds in the sense that a minimizer \mathbf{Z}^* for Problem (18) can be factorized as

$$\mathbf{Z}^* = \mathbf{S}^* \mathbf{B}^H (\mathbf{B}\mathbf{S}^* \mathbf{B}^H + \lambda \mathbf{I})^{-1} \mathbf{Y}, \quad (20)$$

where \mathbf{S}^* is a minimizer for Problem (19).

4.3 Block-Sparse Tensors

In [7], block-sparse core tensors were considered as the natural multidimensional extension of block-sparse vectors in the context of multidimensional data acquisition. The (M_1, \dots, M_Q) block sparsity for a tensor assumes that Q support sets, characterized by M_q indices corresponding to the non-zero entries, fully describe the sparsity pattern of the considered tensor. In the context of compressed sensing with Gaussian measurement matrices, the Cramér-Rao bound (CRB) on the estimation accuracy of a Bernoulli-distributed block-sparse core tensor was also derived in [7]. This prior assumes that each entry of the core tensor has a given probability to be non-zero, leading to random supports of truncated Binomial-distributed cardinalities. Based on the limit form of the Poisson distribution, an approximated CRB expression is provided for large dictionaries and a highly block-sparse core tensor. Using the property that the n -mode unfoldings of a block-sparse tensor follow the multiple-measurement vectors (MMV) model with a joint sparsity pattern, a fast and accurate estimation scheme, called Beamformed mOde based Sparse Estimator (BOSE), is proposed in the second part of [7]. The main contribution of BOSE is to exploit the structure by mapping the MMV model onto the single-measurement vector (SMV) model, via beamforming techniques. Finally, the proposed performance bounds and BOSE are applied in the context of compressed sensing to non-bandlimited multidimensional signals with separable sampling kernels and for multipath channels in a MIMO wireless communication scheme.

4.4 Non-Circularity

Recently, three different sparse recovery strategies have been proposed [46, 52, 51] for exploiting the strict non-circularity property of the impinging signals [49, 50], i.e., the received complex symbols result from real-valued constellations rotated by an arbitrary phase ϕ . As the rotation phase ϕ is usually unknown, the estimation problem becomes a two-dimensional (2-D) sparse recovery problem, which requires estimating the support in the spatial domain as well as in the rotation phase domain.

In [46], a combined 2-D finite dictionary was introduced for both dimensions and the resulting 2-D sparse recovery problem was solved by a $\ell_{2,1}$ -mixed norm relaxation using multiple measurement vectors (MMV). Thereby, the known benefits associated with strictly non-circular (NC) sources [49, 50], e.g., an improved estimation accuracy and a doubling of the number of resolvable signals, can also be achieved via sparse recovery. In order to handle the resulting 2-D off-grid problem, an off-grid estimation procedure was introduced by means of local interpolation.

Article [52] addresses the prohibitive computational complexity required for solving the 2-D mixed-norm problem as a result of sampling both dimensions, significantly increasing the size. Thus, in [52] a sparse optimization framework was proposed based on nuclear norm (rank) minimization after lifting the original optimization problem to a semidefinite programming (SDP) problem in a higher-dimensional space. To this end, the 2-D estimation problem is reduced to a 1-D estimation problem only in the sampled spatial domain, which automatically provides grid-less estimates of the rotation phases. As a result, the proposed method requires a significantly lower computational complexity while providing the same performance benefits. Additionally, an off-grid estimator for the spatial domain has been proposed.

In [51], a grid-less sparse recovery algorithm for NC signals has been proposed

based on atomic norm minimization (ANM). After the NC preprocessing step, the ANM-equivalent SDP problem provides a solution matrix with a two-level Hermitian Toeplitz structure. It was shown that by using the multidimensional generalization of the Vandermonde decomposition, the desired direction estimates can be uniquely extracted from the two-level Hermitian Toeplitz matrix via NC Standard ESPRIT or NC Unitary ESPRIT [16] in closed-form. Due to the exploitation of the NC signal structure, the proposed NC ANM procedure provides a superior estimation accuracy as compared to the original methods for arbitrary signals. In this case, the number of estimated sources can exceed the number of sensors in the array.

5 Mixing Matrix Design

In this section, we consider a noiseless time-invariant version of (2) given as

$$\mathbf{y} = \Phi \mathbf{A} \mathbf{x} = \Psi \mathbf{x} \in \mathbb{C}^N, \quad (21)$$

where $\Psi = \Phi \mathbf{A} \in \mathbb{C}^{N \times P}$ is the total sensing matrix, $\Phi \in \mathbb{C}^{N \times M}$ is the mixing matrix (a.k.a, the projection/compression matrix), $\mathbf{A} \in \mathbb{C}^{M \times P}$ is the dictionary matrix with $P \geq M$, and $\mathbf{x} \in \mathbb{C}^P$ is the signal vector of interest with $\|\mathbf{x}\|_0 \leq s$, i.e., \mathbf{x} is s -sparse. To enhance recoverability of \mathbf{x} , the sensing matrix Ψ should be designed carefully so that it satisfies a certain property (e.g., the NSP or the RIP). Among them, the mutual coherence property of the sensing matrix Ψ , denoted hereafter as $\mu_{\max}(\Psi)$, provides an easy measure with respect to recoverability, which is defined as [40]

$$\mu_{\max}(\Psi) = \max_{i \neq j} \frac{|\psi_i^H \psi_j|}{\|\psi_i\|_2 \|\psi_j\|_2}, \quad (22)$$

with columns $\psi_k = [\psi_{k,1}, \dots, \psi_{k,N}]^T \in \mathbb{C}^N$, $k \in \{1, \dots, P\}$. Clearly, a large coherence $\mu_{\max}(\Psi)$ means that there exist, at least, two highly correlated columns in Ψ , which may confuse any pursuit technique, such as BP and OMP. However, it has been shown that if $s < \frac{1}{2}(1 + 1/\mu_{\max}(\Psi))$, the above techniques are guaranteed to recover \mathbf{x} with high probability [40, 8]. Due to its simplicity, several sensing matrix design methods via mutual coherence minimization have been proposed recently, e.g., in [1, 74, 76]. In general, the results provided by [1, 74, 76] confirm that a well-designed sensing matrix always leads to a better recoverability. However, we note that the achievable mutual coherence by the aforementioned methods is, in general, far from the known theoretical Welch lower-bound, as we will also show in Section 5.3. Moreover, in the scenarios where the mixing matrix is realized using a network of phase shifters, none of the existing methods, to the best of our knowledge, have considered the constant modulus constraints imposed by the mixing matrix hardware that involves cost efficient analog phase shifters.

Formally, by assuming that the dictionary matrix $\mathbf{A} \in \mathbb{C}^{M \times P}$ is given and fixed, sensing matrix design reduces to finding the mixing matrix Φ with constant modulus entries so that the coherence $\mu_{\max}(\Psi)$ is minimized, which can be expressed as

$$\min_{\Phi \in \mathbb{C}^{N \times M}} \mu_{\max}(\Psi) \quad \text{s.t.} \quad \|\psi_k\|_2 = 1 \quad \forall k, \text{ and } |\phi_{k,j}| = 1 \quad \forall k, j. \quad (23)$$

Problem (23) is a non-convex and NP-hard optimization problem [35]. In the following, we propose two solution methods. Subsection 5.1 presents the sequential

mutual coherence minimization (SMCM) we proposed in [5] for the case of $P = M$. In Subsection 5.2, we propose a new method termed enhanced gradient-descent (EGD) for the more general case of $P \geq M$.

5.1 Sensing Matrix Design: $P = M$ Case

In this subsection, we present our first solution to problem (23) for unconstrained mixing matrix design, i.e., by neglecting the constant modulus constraints. Specifically, for a given dictionary matrix $\mathbf{A} \in \mathbb{C}^{M \times P}$, we assume that $P = M$ and the columns of \mathbf{A} are linearly independent so that the condition of $\mathbf{A}\mathbf{A}^{-1} = \mathbf{I}_M$ is guaranteed. In this case, for a given sensing matrix $\Psi \in \mathbb{C}^{N \times P}$ with a coherence $\mu_{\max} = \mu_{\max}(\Psi)$, the optimal unconstrained mixing matrix that preserves μ_{\max} can be obtained as $\Phi_{\text{uncon}} = \Psi\mathbf{A}^{-1} \in \mathbb{C}^{N \times M}$, i.e., $\mu_{\max}(\Phi_{\text{uncon}}\mathbf{A}) = \mu_{\max}$. Therefore, the main task here is to find a low coherence sensing matrix $\Psi \in \mathbb{C}^{N \times P}$.

Let us assume that the columns of Ψ are normalized so that $\|\psi_k\|_2 = 1, \forall k$, and let $\mathbf{G} = \Psi^H\Psi \in \mathbb{C}^{P \times P}$ be the so-called Gram-matrix of Ψ . Moreover, let $\mathbf{G}_{\text{sqr-abs}} \in \mathbb{R}^{P \times P}$ be a matrix so that its (k, j) -th entry is given as $\mathbf{G}_{\text{sqr-abs}}^{[k, j]} = |\mathbf{G}^{[k, j]}|^2$. By expanding $\mathbf{G}_{\text{sqr-abs}}$, it can be expressed as

$$\mathbf{G}_{\text{sqr-abs}} = \begin{bmatrix} |\psi_1^H\psi_1|^2 & \dots & |\psi_1^H\psi_P|^2 \\ \vdots & \ddots & \vdots \\ |\psi_P^H\psi_1|^2 & \dots & |\psi_P^H\psi_P|^2 \end{bmatrix} = \begin{bmatrix} 1 & \dots & |\psi_1^H\psi_P|^2 \\ \vdots & \ddots & \vdots \\ |\psi_P^H\psi_1|^2 & \dots & 1 \end{bmatrix}, \quad (24)$$

which is a symmetric matrix with all ones on its main diagonal. Since all vectors in Ψ have unit norm, we have $\mathbf{G}_{\text{sqr-abs}}^{[k, j]} = |\psi_k^H\psi_j|^2 \leq 1, \forall k \neq j$, and the maximum among them represents the squared-coherence of the matrix Ψ . According to [31, 59], $\mu_{\max}(\Psi)$ has a theoretical lower bound given as $\mu_{\max}(\Psi) \geq \sqrt{\beta}$, where $\beta = \frac{P-N}{N(P-1)}$. This means that, at the best, we have $\mu_{\max}(\Psi) = \sqrt{\beta}$. Noting that the k -th column vector ψ_k appears only in the k -th column and row of $\mathbf{G}_{\text{sqr-abs}}$ (due to its symmetry), we propose to solve problem (23) in an alternating fashion by iterating over the following P subproblems, where the k -th subproblem for updating ψ_k is given as

$$\text{find } \psi_k \in \mathbb{C}^N \quad \text{s.t.} \quad |\psi_j^H\psi_k|^2 \leq \beta \quad \forall j \neq k, \text{ and } \|\psi_k\|_2 = 1. \quad (25)$$

Problems (23) and (25) are related in the sense that both aim to minimize the maximum off-diagonal entry in (24). However, the strict unit-norm constraint $\|\psi_k\|_2 = 1$ in Problem (25) may result in infeasibility for poorly initialized vectors $\psi_j, \forall j \neq k$, especially with a tight lower-bound β . To avoid such a scenario, we propose to relax (25) by dropping the unit-norm constraint and only impose it after a solution is obtained, i.e., we first seek a solution to the following relaxed problem

$$\text{find } \psi_k \in \mathbb{C}^N \quad \text{s.t.} \quad |\psi_j^H\psi_k|^2 \leq \beta \quad \forall j \neq k, \quad (26)$$

which, unlike (25), is guaranteed to be feasible. To obtain a solution of problem (26), a suitable objective function is needed. One possible approach is as follows

$$\psi_k \in \arg \max_{\mathbf{v}_k \in \mathbb{C}^N} |\psi_k^H\mathbf{v}_k|^2 \quad \text{s.t.} \quad |\psi_j^H\mathbf{v}_k|^2 \leq \beta \quad \forall j \neq k, \quad (27)$$

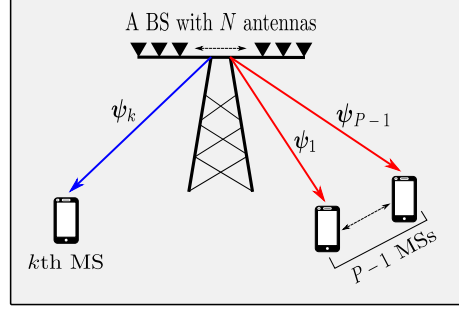


Figure 5: A P -user interference-channel (IC) system model in wireless communication systems, where a base-station (BS) with N antennas serves P single-antenna mobile-stations (MSs) simultaneously so that the data transmission to the k -th MS causes interference to the remaining $P - 1$ MSs.

In problem (27), we borrow the notion from the beamforming design in wireless communication systems, see Fig. 5, where we interpret $\mathbf{v}_k \in \mathbb{C}^N$ as the beamforming vector of the k -th mobile station (MS) that we wish to design so that the desired transmit signal to the k -th MS, i.e., $|\boldsymbol{\psi}_k^H \mathbf{v}_k|^2$, is maximized and the interference signals to the remaining $P - 1$ MSs, i.e., $|\boldsymbol{\psi}_j^H \mathbf{v}_k|^2 \leq \beta, \forall j \neq k$, are minimized for given channel vectors $\{\boldsymbol{\psi}_1, \dots, \boldsymbol{\psi}_P\}$. Due to its convexity, Problem (27) can be efficiently solved using existing techniques, e.g., using the proposed method in [38], as we have shown in [5, 6]. Alternatively, we can resort to the relaxed semidefinite programming (SDP) approach, by dropping the rank-one constraint, and write Problem (27) as

$$\max_{\mathbf{V}_k \in \mathbb{C}^{N \times N}} \text{tr}\{\boldsymbol{\Psi}_k^{\text{cov}} \mathbf{V}_k\} \quad \text{s.t.} \quad \text{tr}\{\boldsymbol{\Psi}_j^{\text{cov}} \mathbf{V}_k\} \leq \beta \quad \forall j \neq k, \text{ and } \mathbf{V}_k \geq 0, \quad (28)$$

where $\boldsymbol{\Psi}_k^{\text{cov}} = \boldsymbol{\psi}_k \boldsymbol{\psi}_k^H \in \mathbb{C}^{N \times N}$ and $\mathbf{V}_k = \mathbf{v}_k \mathbf{v}_k^H \in \mathbb{C}^{N \times N}$. Problem (28) is convex and can be efficiently solved using off-the-shelf solvers, e.g., the CVX toolbox. Let \mathbf{V}_k denote the obtained solution of (28). Then, $\boldsymbol{\psi}_k$ is given by the eigenvector corresponding to the dominant eigenvalue of \mathbf{V}_k , i.e., $\boldsymbol{\psi}_k = \lambda_{\max}\{\mathbf{V}_k\}$. In summary, the proposed mixing matrix design method is given by Algorithm 1. Note that a naïve approach to obtain a constrained mixing matrix, i.e., one with constant modulus entries, is given as $\boldsymbol{\Phi}_{\text{con}} = \boldsymbol{\Pi}(\boldsymbol{\Phi}_{\text{uncon}})$, where $\boldsymbol{\Pi}(\cdot)$ is a projection function that imposes the constant modulus constraints on $\boldsymbol{\Phi}_{\text{uncon}}$ element-wise, i.e., $\boldsymbol{\Pi}(z) = z/|z|$. The performance of such an approach will also be evaluated in Section 5.3.

5.2 Sensing Matrix Design: The General Case

In this subsection, we propose a new solution to (23) for the more general case of $P \geq M$. Similarly to [1], we propose to solve (23) indirectly by solving

$$\min_{\boldsymbol{\Phi} \in \mathbb{C}^{N \times M}} \eta(\boldsymbol{\Phi}) \quad \text{s.t.} \quad \|\boldsymbol{\psi}_k\|_2 = 1 \quad \forall k, \text{ and } |\phi_{k,j}| = 1 \quad \forall k, j, \quad (29)$$

where $\eta(\boldsymbol{\Phi}) = \|\mathbf{A}^H \boldsymbol{\Phi}^H \boldsymbol{\Phi} \mathbf{A} - \mathbf{I}_P\|_F^2$. To obtain a solution for (29), we propose a constrained gradient-descent (GD) method, which updates the mixing matrix $\boldsymbol{\Phi}$

Algorithm 1 Sequential mutual coherence minimization (SMCM)

```

1: Inputs:  $\Psi_{(0)} \in \mathbb{C}^{N \times P}$ . Select  $\epsilon_{\text{th}}$ . Set  $\beta = \frac{P-N}{N(P-1)}$  and  $n = 1$ .
2: for  $n = 1, 2, \dots$  do
3:   for  $k = 1$  to  $P$  do
4:     1: Compute  $\mathbf{V}_{k(n)}$  by solving problem (28).
5:     2: Update the  $k$ -th column vector of  $\Psi_{(n)}$  as  $\psi_{k(n)} = \lambda_{\max} \{\mathbf{V}_{k(n)}\}$ .
6:   end for
7:   if  $\epsilon = |\mu_{\max}(\Psi_{(n)}) - \mu_{\max}(\Psi_{(n-1)})|^2 \leq \epsilon_{\text{th}}$  then
8:     Break
9:   end if
10: end for
11: Output: the sensing matrix  $\Psi$  and the corresponding mixing matrix  $\Phi_{\text{uncon}} = \Psi \mathbf{A}^{-1}$ .

```

iteratively as

$$\Phi_{(n)} = \Pi \left(\Phi_{(n-1)} - \zeta \cdot \frac{\partial \eta(\Phi_{(n-1)})}{\partial \Phi_{(n-1)}} \right), \quad (30)$$

where n is the iteration index, ζ is the step-size, and $\frac{\partial \eta(\Phi_{(n-1)})}{\partial \Phi_{(n-1)}}$ is the gradient of $\eta(\Phi_{(n-1)})$ with respect to $\Phi_{(n-1)}$, which is given as [1]

$$\frac{\partial \eta(\Phi_{(n-1)})}{\partial \Phi_{(n-1)}} = \Phi_{(n-1)} \mathbf{A} (\mathbf{A}^H \Phi_{(n-1)}^H \Phi_{(n-1)} \mathbf{A} - \mathbf{I}_P) \mathbf{A}^H = \Psi_{(n-1)} \mathbf{E}_{(n-1)} \mathbf{A}^H, \quad (31)$$

where $\Psi_{(n-1)} = \Phi_{(n-1)} \mathbf{A}$ and $\mathbf{E}_{(n-1)} = \Psi_{(n-1)}^H \Psi_{(n-1)} - \mathbf{I}_P$. The update step in (30) is a direct extension of the proposed unconstrained GD method in [1] to account for the constant modulus constraints. Our results show that both the unconstrained and the constrained GD-based methods achieve a mutual coherence that is far from the known theoretical Welch lower-bound, as it is shown in Table 1. To enhance their performance, we propose to apply a shrinking operator on the error matrix $\mathbf{E}_{(n-1)}$ entry-wise to get $\tilde{\mathbf{E}}_{(n-1)}$ such that the (k, j) -th entry of $\tilde{\mathbf{E}}_{(n-1)}$ is obtained as

$$\tilde{\mathbf{E}}_{(n-1)}^{[k,j]} = \begin{cases} 0, & |\mathbf{E}_{(n-1)}^{[k,j]}| < \alpha \cdot \sqrt{\beta}, \\ \text{sgn}\{\mathbf{E}_{(n-1)}^{[k,j]}\} \cdot (|\mathbf{E}_{(n-1)}^{[k,j]}| - \alpha \cdot \sqrt{\beta}), & \text{otherwise,} \end{cases} \quad (32)$$

where $\alpha \geq 1$ is an uncertainty measure and β is as defined above. After a closer look at (32), one can see that for a very tight threshold $\tilde{\beta} = \alpha \cdot \sqrt{\beta}$, the resulting error matrix $\tilde{\mathbf{E}}_{(n-1)}$ becomes a sparse matrix, where some of its entries that are smaller than $\tilde{\beta}$ will be set to zero. The direct implication of such a shrinking operator is that the new mixing matrix $\Phi_{(n)}$ will be updated so that it mainly minimizes the entries that are larger than $\tilde{\beta}$. In summary, the proposed enhanced GD (EGD) method for mixing matrix design is given by Algorithm 2. In Section 5.3, we will investigate in detail the impact of α on the performance of EGD method.

5.3 Numerical Results

In this subsection, we present some numerical results for the proposed sensing matrix design methods. In all the simulation results, we set $N = 16$, $M = 64$,

Algorithm 2 Enhanced gradient-descent (EGD)

```

1: Inputs:  $\Phi_{(0)} \in \mathbb{C}^{N \times M}$  and  $\mathbf{A} \in \mathbb{C}^{M \times P}$ . Select  $\epsilon_{\text{th}}$  and  $\zeta$ . Set  $\beta = \frac{P-N}{N(P-1)}$  and  $n = 1$ .
2: Normalize the columns of  $\Psi_{(0)} = \Phi_{(0)}\mathbf{A}$  so that  $\|\psi_{(0),k}\|_2 = 1, \forall k$ .
3: for  $n = 1, 2, \dots$  do
4:   Calculate the error matrix  $\mathbf{E}_{(n-1)} = \Psi_{(n-1)}^H \Psi_{(n-1)} - \mathbf{I}_P$ .
5:   Apply the shrinking operator (32) on  $\mathbf{E}_{(n-1)}$  to get  $\tilde{\mathbf{E}}_{(n-1)}$ .
6:   if mixing matrix should be unconstrained (i.e.,  $\Phi_{\text{uncon}}$ ) then
7:     Compute  $\Phi_{(n)} = \Phi_{(n-1)} - \zeta \cdot \Psi_{(n-1)} \tilde{\mathbf{E}}_{(n-1)} \mathbf{A}^H$ .
8:   else if mixing matrix should be constrained (i.e.,  $\Phi_{\text{con}}$ ) then
9:     Compute  $\Phi_{(n)} = \Pi(\Phi_{(n-1)} - \zeta \cdot \Psi_{(n-1)} \tilde{\mathbf{E}}_{(n-1)} \mathbf{A}^H)$ .
10:  end if
11:  Normalize the columns of  $\Psi_{(n)} = \Phi_{(n)}\mathbf{A}$  so that  $\|\psi_{(n),k}\|_2 = 1, \forall k$ .
12:  if  $\epsilon = |\mu(\Psi_{(n)}) - \mu(\Psi_{(n-1)})| \leq \epsilon_{\text{th}}$  then
13:    Break
14:  end if
15: end for
16: Output: Mixing matrix  $\Phi^*$ 

```

and design the dictionary matrix as $\mathbf{A} = [\mathbf{a}_1, \dots, \mathbf{a}_P] \in \mathbb{C}^{M \times P}$ such that its k -th column is given as $\mathbf{a}_k = [1, e^{j\nu_k}, \dots, e^{j\nu_k(M-1)}]^T \in \mathbb{C}^M$, where $\nu_k = (2\pi(k-1))/P$. For comparison, we include results for a mixing matrix Φ obtained by using the proposed closed-form method in [76]¹, the proposed methods in [74] and [1], as well as randomly, where the entries of Φ are chosen from a zero-mean circularly-symmetric complex Gaussian distribution, termed EVD, Itr-SVD, GD, and Random, respectively. We show the simulation results in terms of the maximum mutual coherence $\mu_{\max}(\Psi)$ defined in (22) and the average mutual coherence $\mu_{\text{avg}}(\Psi)$ defined as

$$\mu_{\text{avg}}(\Psi) = \frac{1}{N_\beta} \left(\sum_{(k,j) \in S_\beta} |\mathbf{G}^{[k,j]}| \right), \quad (33)$$

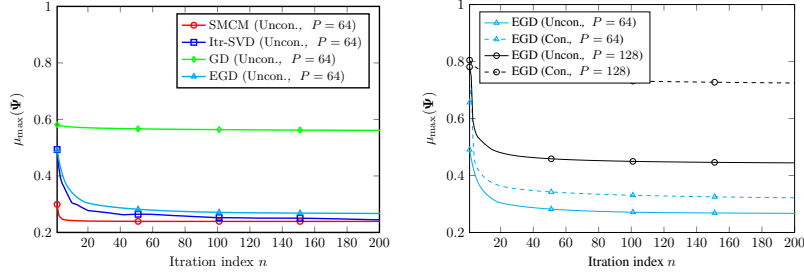
where $S_\beta = \{(k, j) : |\mathbf{G}^{[k,j]}| > \sqrt{\beta}\}$, N_β is the number of elements in the set S_β , and $\mathbf{G} = \Psi^H \Psi$ is the normalized-diagonal Gram matrix. Table 1 shows the obtained results for different values of P . Moreover, Fig. 6 shows the convergence behavior of the iterative methods for the scenarios with $P = 64$ and $P = 128$. For the GD method [1], we use the step-size $\zeta = 5 \times 10^{-4}/n$, while for the EGD method, we use $\zeta = 5 \times 10^{-2}/n$, where n is the iteration index.

From Table 1, when $P = M = 64$, we can see that the SMCM and the Itr-SVD methods achieve similar performance, where the only difference is that SMCM has a faster convergence rate compared to Itr-SVD, as can be seen from Fig. 6. However, as expected, when the ratio P/M increases above 1, the SMCM performance decreases, since the naïve approach of calculating the mixing matrix Φ from the designed sensing matrix Ψ incurs a performance loss. On the other hand, it can be seen that the proposed EGD method has the best performance in almost all of the considered scenarios. Here, we note that the introduced uncertainty measure α has a big impact on the EGD performance and the convergence rate, as can be seen

¹Let $\mathbf{U}\mathbf{\Lambda}\mathbf{U}^H$ be the eigenvalue decomposition of $\mathbf{A}^H\mathbf{A}$. Then, the unconstrained mixing matrix is obtained as $\Phi_{\text{uncon}} = \mathbf{\Lambda}_N^{-1/2} \mathbf{U}_N^H$, where $\mathbf{\Lambda}_N$ and \mathbf{U}_N contain the leading N eigenvalues and eigenvectors, respectively. For constrained mixing matrix scenarios, simply $\Phi_{\text{con}} = \Pi(\Phi_{\text{uncon}})$.

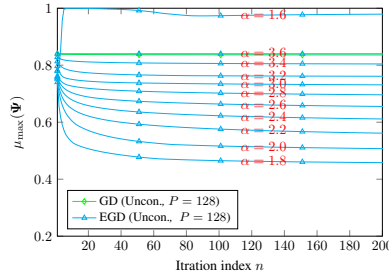
Table 1: Coherence $\mu_{\max}(\Psi)$ ($\mu_{\text{avg}}(\Psi)$) versus P ($N = 16$ and $M = 64$).

	P	Random	EVD	Itr-SVD	GD	EGD	SMCM
Φ_{uncon}	64	0.64 (0.32)	0.56 (0.30)	0.24 (0.23)	0.56 (0.31)	0.26 (0.25) [$\alpha = 1.2$]	0.24 (0.23)
	96	0.74 (0.33)	0.74 (0.32)	0.34 (0.25)	0.67 (0.33)	0.32 (0.30) [$\alpha = 1.4$]	0.53 (0.28)
	128	0.85 (0.34)	0.81 (0.33)	0.50 (0.27)	0.84 (0.34)	0.44 (0.32) [$\alpha = 1.7$]	0.73 (0.32)
Φ_{con}	64	0.64 (0.32)	0.74 (0.32)	0.51 (0.29)	0.64 (0.31)	0.31 (0.27) [$\alpha = 1.3$]	0.57 (0.30)
	96	0.74 (0.33)	0.75 (0.33)	0.67 (0.31)	0.68 (0.33)	0.47 (0.30) [$\alpha = 1.5$]	0.68 (0.33)
	128	0.85 (0.34)	0.82 (0.34)	0.79 (0.33)	0.84 (0.34)	0.72 (0.33) [$\alpha = 1.9$]	0.80 (0.33)


 Figure 6: Coherence $\mu_{\max}(\Psi)$ versus the iteration index.

from Fig. 7. In general, for a sufficiently large α , the EGD converges faster, but its performance degrades and approaches that of the GD. On the other hand, from Fig. 7, we can also note that α should not be too small, since in this case most of the entries within the resulting error matrix $\tilde{\mathbf{E}}$ will be set to zero. From our simulation results in Table 1, we observe that α should be selected so that it is approximately equal to P/M .

In this section, we have proposed the two mixing matrix design methods SMCM and EGD via mutual coherence minimization. For the unconstrained mixing matrix and $P = M$, we have shown that the original nonconvex problem can be relaxed and divided into P convex subproblems, which are updated iteratively using an alternating optimization technique. However, SMCM incurs some performance loss for the constrained case and for $P > M$. To overcome this issue, we have proposed the


 Figure 7: Coherence $\mu_{\max}(\Psi)$ versus the iteration index.

EGD method, which enhances the classical GD-based method of [1] by introducing a shrinking operator on the error matrix. Using computer simulations, we have shown that the proposed SMCM and EGD methods have a faster convergence rate and a lower mutual coherence compared to the benchmark methods.

6 Recovery Algorithms for Nonlinear Measurement Model

This section is devoted recovery techniques that explicitly consider the specific structure of the measurements \mathbf{z} themselves. More specifically, we consider the special case of magnitude only measurements. Hence, we use the information that measurements are nonnegative and we intend to uniquely recover the phase of the measurement signal along with the sparse representation vector.

6.1 Phase Retrieval

In this subsection we consider the phase retrieval problem for a known dictionary \mathbf{A} , which aims to reconstruct an unknown complex-valued signal $\mathbf{x} \in \mathbb{C}^K$ from M noise-corrupted magnitude-only measurements:

$$\mathbf{z} = |\mathbf{Ax}| + \mathbf{n}, \quad (34)$$

where \mathbf{A} is a designed sensing matrix, $\mathbf{n} \in \mathbb{C}^M$ is an additive noise vector, and $|\cdot|$ is applied element-wise. The measurement model (34) can be viewed as a special case of the system depicted in Fig. 1 where Φ is the identity and $\mathcal{T}\{\cdot\} = |\cdot|$. Moreover, the original signal \mathbf{x} is assumed to be sparse. Therefore, the recovery problem can be formulated as the following ℓ_1 regularized nonlinear least-squares:

$$\min_{\mathbf{x} \in \mathbb{C}^K} h(\mathbf{x}) = \underbrace{\frac{1}{2} \|\mathbf{z} - |\mathbf{Ax}|\|_2^2}_{f(\mathbf{x})} + \underbrace{\lambda \|\mathbf{x}\|_1}_{g(\mathbf{x})}. \quad (35)$$

It is a very challenging optimization problem due to the fact that g is nonsmooth and, more notably, f is nonsmooth and nonconvex. Besides, the original signal \mathbf{x} can only be recovered up to a global phase ambiguity as $\mathbf{x} \cdot e^{j\phi}$ preserves both the magnitude measurements and the sparsity pattern.

We solve problem (35) using the STELA algorithm in [71], which is built on the majorization-minimization (MM) techniques in [39] and the block successive convex approximation (BSCA) framework in [65, 72]. The algorithm finds a stationary point of (35) via a sequence of approximate problems that can be solved in parallel. As f in the objective function of (35) is nonconvex and nonsmooth, in each iteration we first construct a smooth upper bound function for f . Then, a descent direction of the upper bound function is obtained by solving a separable convex approximate problem, and a step-size along the descent direction is computed efficiently by exact line search. A decrease of the original objective function h is ensured as its upper bound is decreased. Let $\mathbf{x}^{(l)}$ be the current point in the l -th iteration. Specifically, the algorithm performs the following three steps in each iteration:

1. **Smooth majorization.** The quadratic function f in (35) can be expanded as

$$f(\mathbf{x}) = \frac{1}{2}(\|\mathbf{z}\|_2^2 + \|\mathbf{Ax}\|_2^2) - \mathbf{z}^T \mathbf{Ax}. \quad (36)$$

Further, we note that for any $x \in \mathbb{C}$ and $\phi \in [0, 2\pi)$

$$|x| = |x \cdot e^{j\phi}| \geq \operatorname{Re}\{x \cdot e^{j\phi}\}, \quad (37)$$

and equality holds for $\phi = -\arg(x)$. Thus, defining $\mathbf{z}^{(l)} = \mathbf{z} \odot e^{j\arg(\mathbf{Ax}^{(l)})}$, where $e^{(\cdot)}$ and $\arg(\cdot)$ are applied element-wise and \odot denotes the Hadamard multiplication, we obtain the following smooth and convex upper bound for f in the l -th iteration [39]:

$$\bar{f}^{(l)}(\mathbf{x}) = \frac{1}{2}(\|\mathbf{z}\|_2^2 + \|\mathbf{Ax}\|_2^2) - \mathbf{z}^T \operatorname{Re}\{\mathbf{Ax} \odot e^{-j\arg(\mathbf{Ax}^{(l)})}\} = \frac{1}{2}\|\mathbf{z}^{(l)} - \mathbf{Ax}\|_2^2, \quad (38)$$

which is tight at $\mathbf{x}^{(l)}$, i.e., $\bar{f}^{(l)}(\mathbf{x}^{(l)}) = f(\mathbf{x}^{(l)})$. Consequently, function $\bar{h}^{(l)}(\mathbf{x}) = \bar{f}^{(l)}(\mathbf{x}) + g(\mathbf{x})$ is also an upper bound of the objective function h and tight at $\mathbf{x}^{(l)}$.

2. **Descent direction computation.** Departing from the conventional MM algorithm, we minimize a separable convex approximation of $\bar{h}^{(l)}$, because $\bar{h}^{(l)}$ is computationally too expensive to minimize exactly for our present purpose. Based on the Jacobi algorithm [65], the convex approximate problem in the t -th iteration around point $\mathbf{x}^{(l)}$ is constructed as

$$\tilde{\mathbf{x}}^{(l)} = \operatorname{argmin}_{\mathbf{x} \in \mathbb{C}^K} \sum_{k=1}^K \bar{f}^{(l)}(x_k, \mathbf{x}_{-k}^{(l)}) + g(\mathbf{x}), \quad (39)$$

where \mathbf{x}_{-k} is a $(K-1)$ -dimensional vector obtained by removing the k -th element x_k from \mathbf{x} . Problem (39) is decomposed into K independent subproblems, which can be solved in parallel with suitable hardware [64]. Each subproblem is a Lagrangian form of single-variate LASSO, which admits a closed-form solution. According to [65, Prop. 1], the vector $\tilde{\mathbf{x}}^{(l)} - \mathbf{x}^{(l)}$ represents a descent direction of $\bar{h}^{(l)}$. This motivates us to update $\mathbf{x}^{(l)}$ as follows

$$\mathbf{x}^{(l+1)} = \mathbf{x}^{(l)} + \gamma^{(l)}(\tilde{\mathbf{x}}^{(l)} - \mathbf{x}^{(l)}), \quad (40)$$

where $\gamma^{(l)} \in [0, 1]$ is the step-size. When $\tilde{\mathbf{x}}^{(l)} = \mathbf{x}^{(l)}$, the algorithm has converged to a stationary point of $\bar{h}^{(l)}$, which is also stationary for the original problem (35) [72, Thm. 1].

3. **Step-size computation.** To efficiently find a proper step-size $\gamma^{(l)}$ for the update in (40), we perform an exact line search on a differentiable upper bound of $\bar{h}^{(l)}$ [65]. Thus, the computation of step-size γ^l is formulated as

$$\gamma^{(l)} = \operatorname{argmin}_{0 \leq \gamma \leq 1} \bar{f}^{(l)}(\mathbf{x}^{(l)} + \gamma(\tilde{\mathbf{x}}^{(l)} - \mathbf{x}^{(l)})) + g(\mathbf{x}^{(l)} + \gamma(\tilde{\mathbf{x}}^{(l)} - \mathbf{x}^{(l)})). \quad (41)$$

The line search (41) corresponds to minimizing a convex quadratic function in the interval $[0, 1]$, which can be solved in closed-form. Using the step-size $\gamma^{(l)}$ obtained by the line search (41) in the update (40), a monotonic decrease of the original objective function h in problem (35) is ensured, cf. [71].

The mathematical expressions for the solutions of approximate problem (39) and line search (41) can be further found in [71]. Simulation results with Gaussian random sensing matrix \mathbf{A} are also provided in [71]. The convergence analysis of the BSCA framework is presented in [72]. Besides, several other applications of the BSCA framework can be found in [66, 70, 73, 68, 32, 33]. Furthermore, nonconvex regularization functions can be employed to resolve the defect that the ℓ_1 -regularization tends to produce biased estimates when the sparse signal has large coefficients [69].

6.2 Phase Retrieval with Dictionary Learning

In the previous subsection, we considered the phase retrieval problem for signals that are sparse in the standard basis. However, in some cases, the signals that need to be recovered may only be sparse with respect to an unknown dictionary. Therefore, in this subsection we consider the phase retrieval with dictionary learning problem, which jointly learns a dictionary and sparse representations for reconstructing unknown signals [56, 39, 34].

As one possible application example, we consider a special case of the system depicted in Fig. 1 with a known mixing matrix Φ and $\mathcal{T}\{\cdot\} = |\cdot|$:

$$\mathbf{z}(t) = |\Phi \mathbf{A} \mathbf{x}(t)| + \mathbf{n}(t), \quad t = 1, \dots, D. \quad (42)$$

Given D time samples $\mathbf{Z} = [\mathbf{z}(1), \dots, \mathbf{z}(D)]$, the objective is to jointly recover the unknown sensing matrix \mathbf{A} and sparse transmitted signals $\mathbf{X} = [\mathbf{x}(1), \dots, \mathbf{x}(D)]$. The recovery problem is then formulated as the following phase retrieval with dictionary learning problem [34]:

$$\min_{\mathbf{A} \in \mathcal{A}, \mathbf{X} \in \mathbb{C}^{K \times D}} h(\mathbf{A}, \mathbf{X}) = \underbrace{\frac{1}{2} \|\mathbf{Z} - |\Phi \mathbf{A} \mathbf{X}|\|_2^2}_{f(\mathbf{A}, \mathbf{X})} + \underbrace{\lambda \|\mathbf{X}\|_{1,1}}_{g(\mathbf{X})}. \quad (43)$$

To avoid scaling ambiguities, we restrict \mathbf{A} to be in the convex set $\mathcal{A} = \{\mathbf{A} \in \mathbb{C}^{M \times K} : \|\mathbf{a}_k\|_2 \leq 1, \forall k = 1, \dots, K\}$. Also, $D > K$ is required to avoid trivial solutions.

Analogously, a stationary point of problem (43) can be found by using the majorization technique in (37) and the BSCA framework. In addition to the procedure described in Section 6.1, we also partition the variables into two blocks, i.e., \mathbf{A} and \mathbf{X} , and select a given number $k_B \in \{1, 2\}$ of block variables to update in each iteration. The block variables can be selected by cyclic or random update rules [72].

Let $(\mathbf{A}^{(l)}, \mathbf{X}^{(l)})$ be the current point in the l -th iteration. We first consider the case where both block variables \mathbf{A} and \mathbf{X} are selected to update. Then, the three main steps that are performed in each iteration by the BSCA-based algorithm for problem (43) are outlined as follows:

1. **Smooth majorization.** Exploiting the same majorization technique given in (37), we construct a smooth upper bound for f in (43). Defining $\mathbf{Z}^{(l)} = \mathbf{Z} \odot e^{j \arg(\Phi \mathbf{A} \mathbf{X}^{(l)})}$, we can obtain the following smooth upper bound for f in the l -th iteration:

$$\tilde{f}^{(l)}(\mathbf{A}, \mathbf{X}) = \frac{1}{2} \|\mathbf{Z}^{(l)} - \Phi \mathbf{A} \mathbf{X}\|_F^2, \quad (44)$$

which is tight at $(\mathbf{A}^{(l)}, \mathbf{X}^{(l)})$. Similarly, we construct function $\tilde{h}^{(l)}(\mathbf{A}, \mathbf{X}) = \tilde{f}^{(l)}(\mathbf{A}, \mathbf{X}) + g(\mathbf{X})$ as an upper bound of the objective function h which is

tight at $(\mathbf{A}^{(l)}, \mathbf{X}^{(l)})$. However, we remark that, unlike in Section 6.1, the upper bound function $\bar{f}^{(l)}$ in (44) is nonconvex due to the bilinear terms $\mathbf{A}\mathbf{X}$. Therefore, the convex approximation in the next step becomes necessary for efficiently finding a descent direction.

2. **Descent direction computation.** Based on the Jacobi algorithm [65], the separable convex approximation for the minimization of $\bar{h}^{(l)}$ is constructed as

$$(\tilde{\mathbf{A}}^{(l)}, \tilde{\mathbf{X}}^{(l)}) \in \operatorname{argmin}_{\mathbf{A} \in \mathcal{A}, \mathbf{X}} \left\{ \begin{array}{l} \sum_{m=1}^M \sum_{k=1}^K \bar{f}^{(l)}(x_{mk}, \mathbf{A}^{(l)}, \mathbf{X}_{-mk}^{(l)}) \\ + \sum_{m=1}^M \bar{f}^{(l)}(\mathbf{a}_k, \mathbf{A}_{-k}^{(l)}, \mathbf{X}^{(l)}) + g(\mathbf{X}) \end{array} \right\}, \quad (45)$$

where \mathbf{A}_{-k} is an $M \times (K-1)$ matrix obtained by removing the k -th column \mathbf{a}_k from \mathbf{A} and \mathbf{X}_{-mk} denotes the collection of all entries of \mathbf{X} except the (m, k) -th entry x_{mk} . Problem (35) can be decomposed into $K + (K \times D)$ independent subproblems. Each subproblem can be solved either in closed-form or by an efficient algorithm. Then, the difference $(\tilde{\mathbf{A}}^{(l)} - \mathbf{A}^{(l)}, \tilde{\mathbf{X}}^{(l)} - \mathbf{X}^{(l)})$ represents a descent direction of $\bar{h}^{(l)}$ in the domain of problem (43). Defining $\Delta \mathbf{A} = \tilde{\mathbf{A}}^{(l)} - \mathbf{A}^{(l)}$ and $\Delta \mathbf{X} = \tilde{\mathbf{X}}^{(l)} - \mathbf{X}^{(l)}$, the following simultaneous update rule can be applied:

$$\mathbf{A}^{(l+1)} = \mathbf{A}^{(l)} + \gamma^{(l)} \Delta \mathbf{A} \quad \text{and} \quad \mathbf{X}^{(l+1)} = \mathbf{X}^{(l)} + \gamma^{(l)} \Delta \mathbf{X}, \quad (46)$$

with a proper step-size $\gamma^{(l)} \in [0, 1]$. When $(\tilde{\mathbf{A}}^{(l)}, \tilde{\mathbf{X}}^{(l)}) = (\mathbf{A}^{(l)}, \mathbf{X}^{(l)})$, the algorithm has converged to a stationary point of $\bar{h}^{(l)}$, which is also stationary for the original problem (43) [72, Thm. 1].

3. **Step-size computation.** We perform an exact line search on a differentiable upper bound of $\bar{h}^{(l)}$ to efficiently find a step-size $\gamma^{(l)}$ that ensures a monotonic decrease of the original objective function h in (43). The computation of step-size $\gamma^{(l)}$ is then formulated as

$$\gamma^{(l)} = \operatorname{argmin}_{0 \leq \gamma \leq 1} \left\{ \begin{array}{l} \bar{f}^{(l)}(\mathbf{A}^{(l)} + \gamma \Delta \mathbf{A}, \mathbf{X}^{(l)} + \gamma \Delta \mathbf{X}) \\ + g(\mathbf{X}^{(l)} + \gamma (\tilde{\mathbf{X}}^{(l)} - \mathbf{X}^{(l)})) \end{array} \right\}. \quad (47)$$

Problem (47) can be solved by rooting its derivative, a third-order polynomial, which admits a closed-form expression.

In contrast to the above joint update case, if only one block variable is selected to update in the l -th iteration, then we solve the approximate problem (45) only with respect to the selected block variable, which requires solving only the corresponding subproblems. Moreover, the update (46) is also performed only on the selected block variable, which is equivalent to setting the difference of the non-selected block variable to be all-zero. Further, when either of the matrices $\Delta \mathbf{A}$ and $\Delta \mathbf{X}$ is all-zero, the line search problem (47) reduces to a simple convex quadratic program.

Details of the BSCA-based algorithm for phase retrieval with dictionary learning and results from numerical experiments can further be found in [34].

7 Conclusions

Compressed sensing (CS) is a powerful technique for estimating sparse signals, which can be recovered, under mild conditions, from far fewer samples than otherwise indicated by the Nyquist-Shannon sampling theorem. Moreover, it was

observed that incorporating side constraints not only improves the recovery guarantees but also reduces the required number of samples. This chapter builds on this important observation by addressing sparse signal reconstruction under various types of structural side constraints, including integrality, constant modulus, row and rank sparsity, and strict non-circularity constraints. Moreover, this chapter addresses the measurement system design for linear and nonlinear measurements of sparse signals. For the linear measurement systems, two mixing matrix design methods based on mutual coherence minimization are proposed, where constant modulus constraints are imposed element-wise to satisfy the mixing matrix hardware that involves cost-efficient analog phase shifters. For nonlinear measurement systems, parallel optimization design algorithms are proposed to efficiently compute the stationary points in the sparse phase retrieval problem with and without dictionary learning.

References

- [1] Abolghasemi, V., Ferdowsi, S., Makkiabadi, B., Sanei, S.: On optimization of the measurement matrix for compressive sensing. In: Proc. 18th European Signal Processing Conference, pp. 427–431 (2010)
- [2] Ardah, K., d. Almeida, A.L.F., Haardt, M.: Low-complexity millimeter wave CSI estimation in MIMO-OFDM hybrid beamforming systems. In: WSA 2019; 23rd International ITG Workshop on Smart Antennas, pp. 1–5 (2019)
- [3] Ardah, K., de Almeida, A.L.F., Haardt, M.: A gridless CS approach for channel estimation in hybrid massive MIMO systems. In: 2019 IEEE International Conference on Acoustics, Speech and Signal Processing (ICASSP), pp. 4160–4164 (2019)
- [4] Ardah, K., Gharekhloo, S., de Almeida, A.L.F., Haardt, M.: TRICE: A channel estimation framework for RIS-aided millimeter-wave MIMO systems. *IEEE Signal Process. Lett.* **28**, 513–517 (2021)
- [5] Ardah, K., Pesavento, M., Haardt, M.: A novel sensing matrix design for compressed sensing via mutual coherence minimization. In: 2019 IEEE 8th International Workshop on Computational Advances in Multi-Sensor Adaptive Processing (CAMSAP), pp. 66–70 (2019)
- [6] Ardah, K., Sokal, B., de Almeida, A.L.F., Haardt, M.: Compressed sensing based channel estimation and open-loop training design for hybrid analog-digital massive MIMO systems. In: 2020 IEEE International Conference on Acoustics, Speech and Signal Processing (ICASSP), pp. 4597–4601 (2020)
- [7] Boyer, R., Haardt, M.: Noisy compressive sampling based on block-sparse tensors: Performance limits and beamforming techniques. *IEEE Trans. Signal Process.* (23), 6075–6088 (2016)
- [8] Choi, J.W., Shim, B., Ding, Y., Rao, B., Kim, D.I.: Compressed sensing for wireless communications: Useful tips and tricks. *IEEE Commun. Surveys Tuts.* **19**(3), 1527–1550 (2017)
- [9] Fischer, T., Hegde, G., Matter, F., Pesavento, M., Pfetsch, M.E., Tillmann, A.M.: Joint antenna selection and phase-only beamforming using mixed-integer nonlinear programming. In: WSA 2018; 22nd International ITG Workshop on Smart Antennas, pp. 1–7 (2018)

- [10] Fischer, T., Pfetsch, M.E.: Monoidal cut strengthening and generalized mixed-integer rounding for disjunctive programs. *Oper. Res. Lett.* **45**(6), 556–560 (2017)
- [11] Fischer, T., Pfetsch, M.E.: Branch-and-cut for linear programs with overlapping SOS1 constraints. *Math. Prog. Comp.* **10**(1), 33–68 (2018)
- [12] Foucart, S., Rauhut, H.: A Mathematical Introduction to Compressive Sensing. *Appl. Numer. Harmon. Anal.* Birkhäuser/Springer, New York (2013)
- [13] Gao, F., Tian, Z., Larsson, E.G., Pesavento, M., Jin, S.: Introduction to the special issue on array signal processing for angular models in massive MIMO communications. *IEEE J. Sel. Topics Signal Process.* **13**(5), 882–885 (2019)
- [14] Gribonval, R., Nielsen, M.: Sparse representations in unions of bases. *IEEE Trans. Inf. Theory* **49**(12), 3320–3325 (2003)
- [15] Haardt, M., Pesavento, M., Roemer, F., El Korso, M.N.: Subspace methods and exploitation of special array structures. In: A.M. Zoubir, M. Viberg, R. Chellappa, S. Theodoridis (eds.) *Academic Press Library in Signal Processing: Volume 3 – Array and Statistical Signal Processing*, pp. 651–717. Elsevier (2014). Chapter 15
- [16] Haardt, M., Roemer, F.: Enhancements of Unitary ESPRIT for non-circular sources. In: 2004 IEEE International Conference on Acoustics, Speech, and Signal Processing (ICASSP), vol. II, pp. 101–104. Montreal, Canada (2004)
- [17] Hegde, G., Pesavento, M., Pfetsch, M.E.: Joint active device identification and symbol detection using sparse constraints in massive MIMO systems. In: 2017 25th European Signal Processing Conference (EUSIPCO), pp. 703–707. IEEE (2017)
- [18] Hegde, G., Yang, Y., Steffens, C., Pesavento, M.: Parallel low-complexity M-PSK detector for large-scale MIMO systems. In: 2016 IEEE Sensor Array and Multichannel Signal Processing Workshop (SAM), pp. 1–5. IEEE (2016)
- [19] Heuer, J., Matter, F., Pfetsch, M.E., Theobald, T.: Block-sparse recovery of semidefinite systems and generalized null space conditions. *Linear Algebra Appl.* **603**, 470–495 (2020)
- [20] Hyder, M.M., Mahata, K.: Direction-of-arrival estimation using a mixed $\ell_{2,0}$ norm approximation. *IEEE Trans. Signal Process.* **58**(9), 4646–4655 (2010)
- [21] Juditsky, A., Karzan, F.K., Nemirovski, A.: On a unified view of nullspace-type conditions for recoveries associated with general sparsity structures. *Linear Algebra Appl.* **441**, 124–151 (2014)
- [22] Keiper, S., Kutyniok, G., Lee, D.G., Pfander, G.E.: Compressed sensing for finite-valued signals. *Linear Algebra Appl.* **532**, 570–613 (2017)
- [23] Khajehnejad, M.A., Dimakis, A.G., Xu, W., Hassibi, B.: Sparse recovery of nonnegative signals with minimal expansion. *IEEE Trans. Signal Process.* **59**(1), 196–208 (2011)
- [24] Kong, L., Sun, J., Xiu, N.: S-semigoodness for low-rank semidefinite matrix recovery. *Pac. J. Optim.* **10**(1), 73–83 (2014)
- [25] Kowalski, M.: Sparse regression using mixed norms. *Appl. Comput. Harmon. Anal.* **27**(3), 303–324 (2009)

- [26] Krim, H., Viberg, M.: Two decades of array signal processing research: the parametric approach. *IEEE Signal Process. Mag.* **13**(4), 67–94 (1996)
- [27] Kushe, G., Yang, Y., Pesavento, M.: A block successive convex approximation framework for multidimensional harmonic retrieval and imperfect measurements. In: *WSA 2020; 24th International ITG Workshop on Smart Antennas*, pp. 1–5 (2020)
- [28] Kushe, G., Yang, Y., Steffens, C., Pesavento, M.: A parallel sparse regularization method for structured multilinear low-rank tensor decomposition. In: *2019 27th European Signal Processing Conference (EUSIPCO)*, pp. 1–5 (2019)
- [29] Kuske, J., Swoboda, P., Petra, S.: A novel convex relaxation for non-binary discrete tomography. In: *International Conference on Scale Space and Variational Methods in Computer Vision*, pp. 235–246. Springer (2017)
- [30] Lange, J.H., Pfetsch, M.E., Seib, B.M., Tillmann, A.M.: Sparse recovery with integrality constraints. *Discrete Applied Math.* **283**, 346–366 (2020)
- [31] Li, X., Ye, J., Li, G., Bai, H., Jiang, Q.: A new approach to sensing matrix optimization using steepest descent algorithm. In: *2015 34th Chinese Control Conference (CCC)*, pp. 4939–4944 (2015)
- [32] Liu, T., Hoang, M.T., Yang, Y., Pesavento, M.: A block coordinate descent algorithm for sparse gaussian graphical model inference with laplacian constraints. In: *2019 IEEE 8th International Workshop on Computational Advances in Multi-Sensor Adaptive Processing (CAMSAP)*, pp. 236–240 (2019)
- [33] Liu, T., Hoang, M.T., Yang, Y., Pesavento, M.: A parallel optimization approach on the infinity norm minimization problem. In: *2019 27th European Signal Processing Conference (EUSIPCO)*, pp. 1–5. IEEE (2019)
- [34] Liu, T., Tillmann, A.M., Yang, Y., Eldar, Y.C., Pesavento, M.: A parallel algorithm for phase retrieval with dictionary learning. In: *2021 IEEE International Conference on Acoustics, Speech and Signal Processing (ICASSP)* (2021)
- [35] Lu, C., Li, H., Lin, Z.: Optimized projections for compressed sensing via direct mutual coherence minimization. *Signal Processing* **151**, 45–55 (2018)
- [36] Malioutov, D., Çetin, M., Willsky, A.: A sparse signal reconstruction perspective for source localization with sensor arrays. *IEEE Trans. Signal Process.* **53**(8), 3010–3022 (2005)
- [37] Oymak, S., Hassibi, B.: New null space results and recovery thresholds for matrix rank minimization. In *Proc. ISIT 2011*, Preprint arXiv:1011.6326 (2010)
- [38] Park, J., Lee, G., Sung, Y., Yukawa, M.: Coordinated beamforming with relaxed zero forcing: The sequential orthogonal projection combining method and rate control. *IEEE Trans. Signal Process.* **61**(12), 3100–3112 (2013)
- [39] Qiu, T., Palomar, D.P.: Undersampled sparse phase retrieval via majorization-minimization. *IEEE Trans. Signal Process.* **65**(22), 5957–5969 (2017)
- [40] Rani, M., Dhok, S.B., Deshmukh, R.B.: A systematic review of compressive sensing: Concepts, implementations and applications. *IEEE Access* **6**, 4875–4894 (2018)

- [41] Steffens, C., Pesavento, M.: Block- and rank-sparse recovery for direction finding in partly calibrated arrays. *IEEE Trans. Signal Process.* **66**(2), 384–399 (2018)
- [42] Steffens, C., Pesavento, M.: Collaborative Sensing Techniques, chap. 7, pp. 121–145. John Wiley & Sons, Ltd (2020)
- [43] Steffens, C., Pesavento, M., Pfetsch, M.E.: A compact formulation for the $\ell_{2,1}$ mixed-norm minimization problem. *IEEE Trans. Signal Process.* **66**(6), 1483–1497 (2018)
- [44] Steffens, C., Suleiman, W., Sorg, A., Pesavento, M.: Gridless compressed sensing under shift-invariant sampling. In: 2017 IEEE International Conference on Acoustics, Speech and Signal Processing (ICASSP), pp. 4735–4739 (2017)
- [45] Steffens, C., Yang, Y., Pesavento, M.: Multidimensional sparse recovery for MIMO channel parameter estimation. In: 2016 24th European Signal Processing Conference (EUSIPCO), pp. 66–70 (2016)
- [46] Steinwandt, J., Roemer, F., Haardt, M.: Sparsity-based direction-of-arrival estimation for strictly non-circular sources. In: 2016 IEEE International Conference on Acoustics, Speech, and Signal Processing (ICASSP). Shanghai, China (2016)
- [47] Steinwandt, J., Roemer, F., Haardt, M.: Generalized least squares for ESPRIT-type direction of arrival estimation. *IEEE Signal Process. Lett.* **24**(11), 1681–1685 (2017)
- [48] Steinwandt, J., Roemer, F., Haardt, M.: Performance analysis of ESPRIT-type algorithms for co-array structures. In: 2017 IEEE 7th International Workshop on Computational Advances in Multi-Sensor Adaptive Processing (CAMSAP), pp. 1–5 (2017)
- [49] Steinwandt, J., Roemer, F., Haardt, M., Del Galdo, G.: Deterministic Cramér-Rao bound for strictly non-circular sources and analytical analysis of the achievable gains. *IEEE Trans. Signal Process.* **64**(17), 4417–4431 (2016)
- [50] Steinwandt, J., Roemer, F., Haardt, M., Del Galdo, G.: Performance analysis of multi-dimensional ESPRIT-type algorithms for arbitrary and strictly non-circular sources with spatial smoothing. *IEEE Trans. Signal Process.* **65**(9), 2262–2276 (2017)
- [51] Steinwandt, J., Roemer, F., Steffens, C., Haardt, M., Pesavento, M.: Gridless superresolution direction finding for strictly non-circular sources based on atomic norm minimization. In: 2016 50th Asilomar Conference on Signals, Systems, and Computers. Pacific Grove, CA (2016)
- [52] Steinwandt, J., Steffens, C., Pesavento, M., Haardt, M.: Sparsity-aware direction finding for strictly non-circular sources based on rank minimization. In: 2016 IEEE Sensor Array and Multichannel Signal Processing Workshop (SAM). Rio de Janeiro, Brazil (2016)
- [53] Stojnic, M.: Recovery thresholds for ℓ_1 optimization in binary compressed sensing. In: 2010 IEEE International Symposium on Information Theory, pp. 1593–1597. IEEE (2010)
- [54] Stojnic, M., Parvaresh, F., Hassibi, B.: On the reconstruction of block-sparse signals with an optimal number of measurements. *IEEE Trans. Signal Process.* **57**(8), 3075–3085 (2009)

- [55] Suleiman, W., Steffens, C., Sorg, A., Pesavento, M.: Gridless compressed sensing for fully augmentable arrays. In: 2017 25th European Signal Processing Conference (EUSIPCO), pp. 1986–1990 (2017)
- [56] Tillmann, A.M., Eldar, Y.C., Mairal, J.: DOLPHIn – dictionary learning for phase retrieval. *IEEE Trans. Signal Process.* **64**(24), 6485–6500 (2016)
- [57] Tillmann, A.M., Pfetsch, M.E.: The computational complexity of the restricted isometry property, the nullspace property, and related concepts in compressed sensing. *IEEE Trans. Inf. Theory* **60**(2), 1248–1259 (2014)
- [58] Tropp, J.A.: Algorithms for simultaneous sparse approximation. Part II: Convex relaxation. *Signal Processing* **86**(3), 589–602 (2006)
- [59] Tropp, J.A., Dhillon, I.S., Heath, R.W., Strohmer, T.: Designing structured tight frames via an alternating projection method. *IEEE Trans. Inf. Theory* **51**(1), 188–209 (2005)
- [60] Turlach, B.A., Venables, W.N., Wright, S.J.: Simultaneous variable selection. *Technometrics* **47**(3), 349–363 (2005)
- [61] Van Trees, H.L.: *Optimum Array Processing*. Wiley, New York (2002)
- [62] Vigerske, S.: *Decomposition in multistage stochastic programming and a constraint integer programming approach to mixed-integer nonlinear programming*. Ph.D. thesis, Humboldt-Universität zu Berlin (2013)
- [63] Walewski, A.C., Steffens, C., Pesavento, M.: Off-grid parameter estimation based on joint sparse regularization. In: SCC 2017; 11th International ITG Conference on Systems, Communications and Coding, pp. 1–6 (2017)
- [64] Wang, X., Liu, T., Trinh-Hoang, M., Pesavento, M.: GPU-accelerated parallel optimization for sparse regularization. In: 2020 IEEE 11th Sensor Array and Multichannel Signal Processing Workshop (SAM), pp. 1–5 (2020)
- [65] Yang, Y., Pesavento, M.: A unified successive pseudoconvex approximation framework. *IEEE Trans. Signal Process.* **65**(13), 3313–3328 (2017)
- [66] Yang, Y., Pesavento, M.: Energy efficiency in MIMO interference channels: Social optimality and max-min fairness. In: 2018 IEEE International Conference on Acoustics, Speech and Signal Processing (ICASSP), pp. 3689–3693 (2018)
- [67] Yang, Y., Pesavento, M.: A parallel best-response algorithm with exact line search for nonconvex sparsity-regularized rank minimization. In: 2018 IEEE International Conference on Acoustics, Speech and Signal Processing (ICASSP), pp. 6323–6327 (2018)
- [68] Yang, Y., Pesavento, M., Chatzinotas, S., Ottersten, B.: Parallel and hybrid soft-thresholding algorithms with line search for sparse nonlinear regression. In: *European Signal Processing Conference*, vol. 2018-Sept, pp. 1587–1591 (2018)
- [69] Yang, Y., Pesavento, M., Chatzinotas, S., Ottersten, B.: Successive convex approximation algorithms for sparse signal estimation with nonconvex regularizations. *IEEE J. Sel. Topics Signal Process.* **12**(6), 1286–1302 (2018)
- [70] Yang, Y., Pesavento, M., Chatzinotas, S., Ottersten, B.: Energy efficiency optimization in MIMO interference channels: A successive pseudoconvex approximation approach. *IEEE Trans. Signal Process.* **67**(15), 4107–4121 (2019)

- [71] Yang, Y., Pesavento, M., Eldar, Y.C., Ottersten, B.: Parallel coordinate descent algorithms for sparse phase retrieval. In: 2019 IEEE International Conference on Acoustics, Speech and Signal Processing (ICASSP), pp. 7670–7674 (2019)
- [72] Yang, Y., Pesavento, M., Luo, Z.Q., Ottersten, B.: Inexact block coordinate descent algorithms for nonsmooth nonconvex optimization. *IEEE Trans. Signal Process.* **68**, 947–961 (2020)
- [73] Yang, Y., Pesavento, M., Zhang, M., Palomar, D.P.: An online parallel algorithm for recursive estimation of sparse signals. *IEEE Trans. Signal Inf. Process. Netw.* **2**(3), 290–305 (2016)
- [74] Yu, L., Li, G., Chang, L.: Optimizing projection matrix for compressed sensing systems. In: 2011 8th International Conference on Information, Communications Signal Processing (ICICSP), pp. 1–5 (2011)
- [75] Yuan, M., Lin, Y.: Model selection and estimation in regression with grouped variables. *J. R. Stat. Soc. Series B (Statistical Methodology)* **68**(1), 49–67 (2006)
- [76] Zelnik-Manor, L., Rosenblum, K., Eldar, Y.C.: Sensing matrix optimization for block-sparse decoding. *IEEE Trans. Signal Process.* **59**(9), 4300–4312 (2011)
- [77] Zhang, Y.: A simple proof for recoverability of ℓ_1 -minimization (II): the nonnegativity case. Technical report TR05-10, Dept. of Computational and Applied Mathematics, Rice University (2005)